

CHAPTER 4

Results

4.1 Morphological description of adult

All measurements of adult worms based on 30 whole-mount specimens from *Bos taurus* and *Bubalus bubalis*. Body large and leaf-like shaped, dorso-ventrally flattened, with 39.00-49.50 (44.40 in average) mm in length and 9.50-12.50 (1.11 in average) mm in width. Head become prominent cephalic cone. The entire body was covered with scale-like spines, excepted around with oral and ventral suckers and theirs spines were mostly dome shape, with finger-like protrusions at tip. Oral and ventral suckers rounded and well developed, usually close together on the cephalic cone. Oral sucker opened sub-terminal, usually smaller than ventral sucker, with 0.55-1.28 (1.00 in average) mm in length and 0.50-1.05 (0.78 in average) mm in width. Ventral sucker rounded 1.38-2.13 (1.70 in average) mm in length and 1.31-2.00 (1.62 in average) mm in width. The muscular of oral and ventral suckers were well developed. Prepharynx presented and shorted. Pharynx shorted and well developed with 0.45-1.00 (0.83 in average) mm in length and 0.43-0.78 (0.60 in average) mm in width. Esophagus usually shorted and genital pore is at the basal of cephalic cone. Intestines absolutely branched and extended laterally. Two highly dendritic testes arranged tandemly and occupied post-ovarian area between vitelline fields. One branched ovary, situated sub-median, anterior to testes. Diffusely branched and well developed vitelline follicles, extended laterally. Uterus shorted and convoluted shaped, situated between ventral sucker and ovary (Figs. 4.1-4.2).

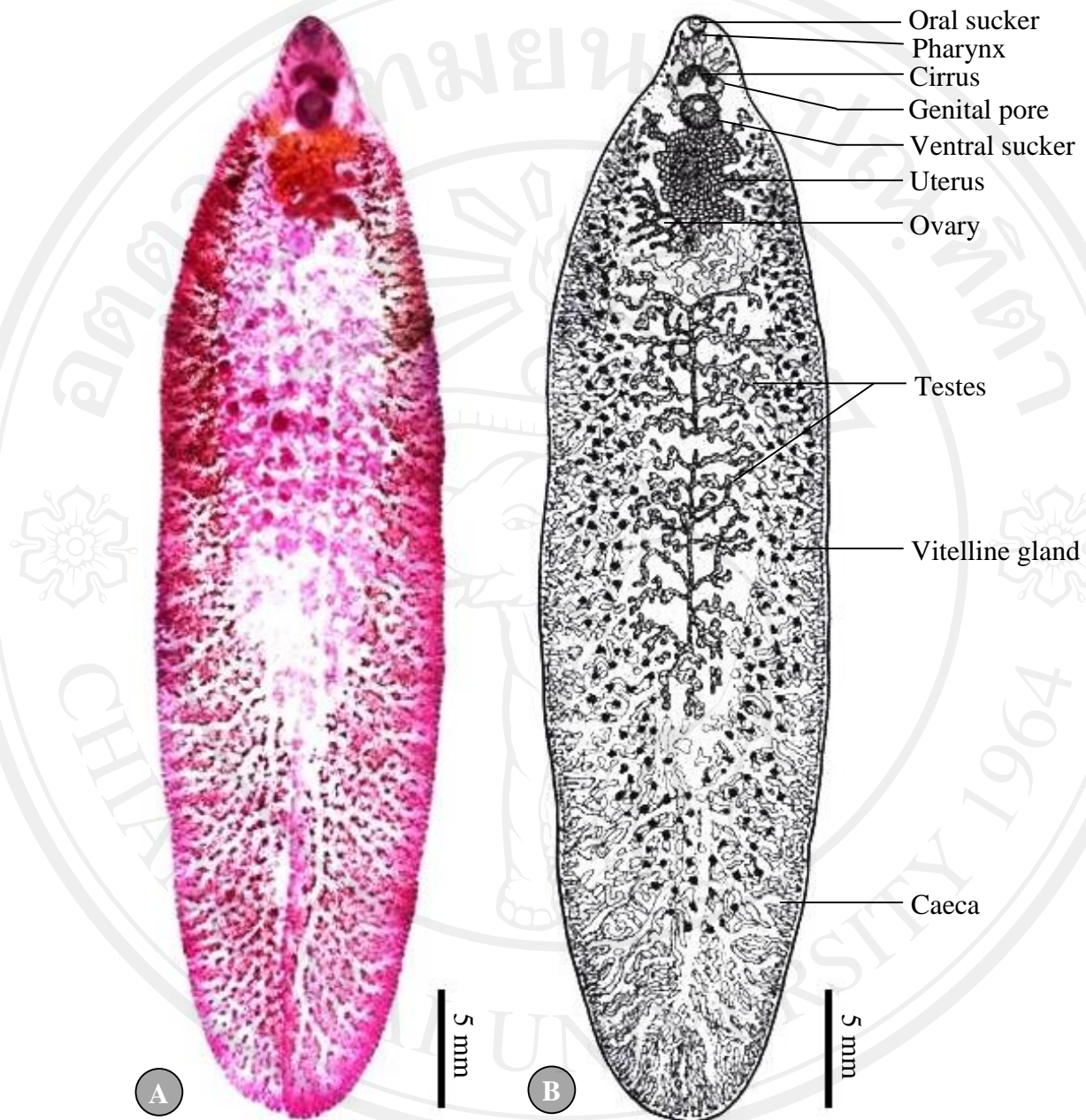


Figure 4.1 Illustration demonstrated the morphology of *F. gigantica* adults from *Bos taurus* and *Bubalus bubalis*; (A) photographs of permanent slide, (B) drawing

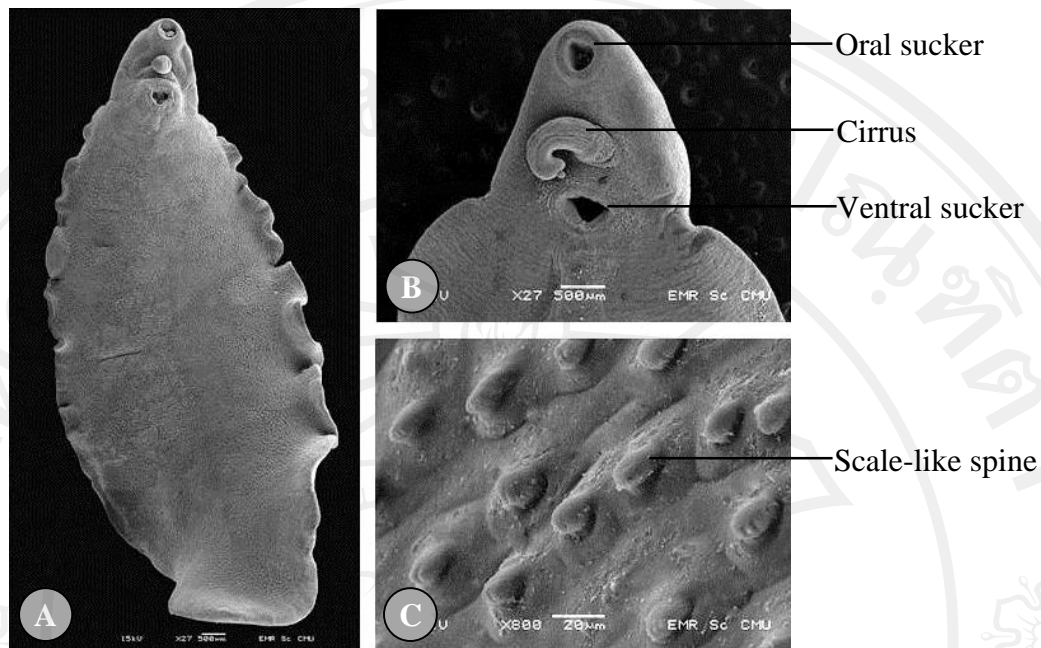


Figure 4.2 SEM photographs demonstrated the morphology of *F. gigantica* adults from *Bos taurus* and *Bubalus bubalis*; (A) the whole worm of *F. gigantica*, (B) the cirrus, oral and ventral sucker, (C) the scale-like spine showing finger-like protrusions at tip

4.2 The prevalence of adult worm infection

The flukes were collected in liver and gallbladder of *Bubalus bubalis* and *Bos taurus* in 3 slaughterhouses from Mueang, Doi Saket, and San Pa Tong districts of Chiang Mai province, during October 2010 to September 2012. Fifty five of *Bubalus bubalis* and 51 of *Bos taurus* were examined. The infection of *F. gigantica* in *Bubalus bubalis* were highest than *Bos taurus*, total prevalence of infection were 67.27% and 52.94%, respectively. The highest to lowest prevalence of *F. gigantica* in both *Bubalus bubalis* and *Bos taurus* were also recorded from Doi Saket, Mueang, and San Pa Tong districts. The prevalence of *F. gigantica* infection in *Bubalus bubalis* were 81.25% (13/16), 62.50% (15/24) and 60.00% (9/15), respectively. In *Bos taurus*, the prevalence of infection were 62.50% (10/16), 50.00% (9/18) and 47.06% (8/17), respectively (Fig. 4.3).

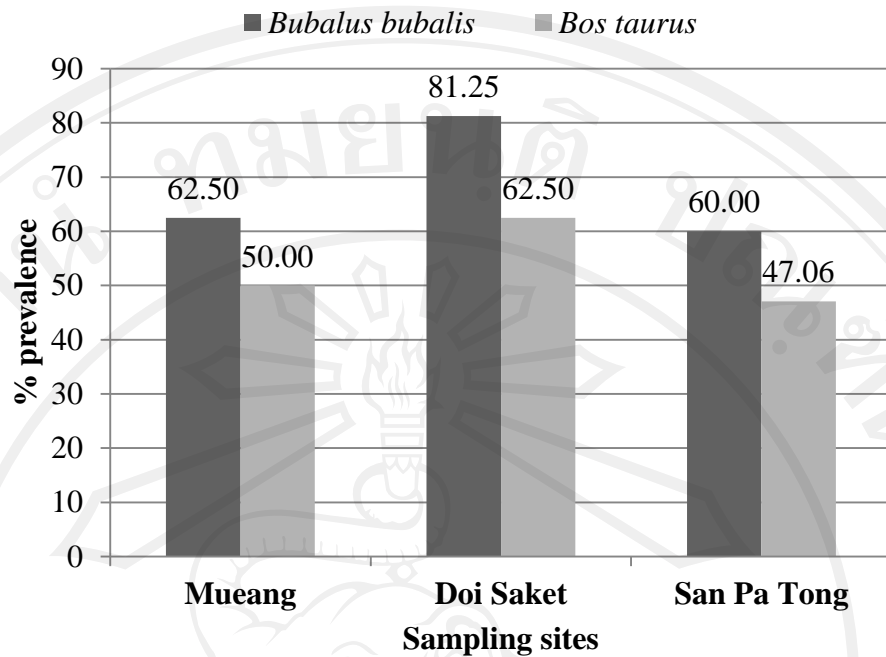


Figure 4.3 The prevalence of *F.gigantica* adults infection recovered in *Bubalus bubalis* and *Bos taurus* of Mueang, Doi Saket, and San Pa Tong districts of Chiang Mai Province

4.3 The prevalence of cercarial infection of snail intermediate hosts in natural sampling sites

A total of 867 snails belonging to 14 species were investigated for the presence of cercariae. Fourteen species of snail intermediate hosts were *Bithynia siamensis*, *Brotia costula costula*, *Brotia citrina*, *Brotia baccata*, *Eyriesia eyriesi*, *Filopaludina martensi martensi*, *F. dorliaris*, *F. polygamma*, *Lymnaea auricularia rubiginosa*, *Melanoides tuberculata*, *M. jugicostis*, *Physa acuta*, *Tarebia granifera*, *Thiara scabra* were collected. The 8 types of cercariae as parapleurolophocercous cercaria, pleurolophocercous cercaria, monostome cercaria, distome cercaria, xiphidiocercaria, echinostome cercaria, transversotremacercaria and furcocercous cercaria were recorded (Appendix A).

The highest total prevalence of cercarial infection in each sampling site was observed in Mae Taeng district with 38.16%, followed by the Chom Thong and Mae Rim districts with 26.95%, and 23.53%, respectively. The lowest total prevalence was recorded in Phrao district, with 11.76% (Fig. 4.4).

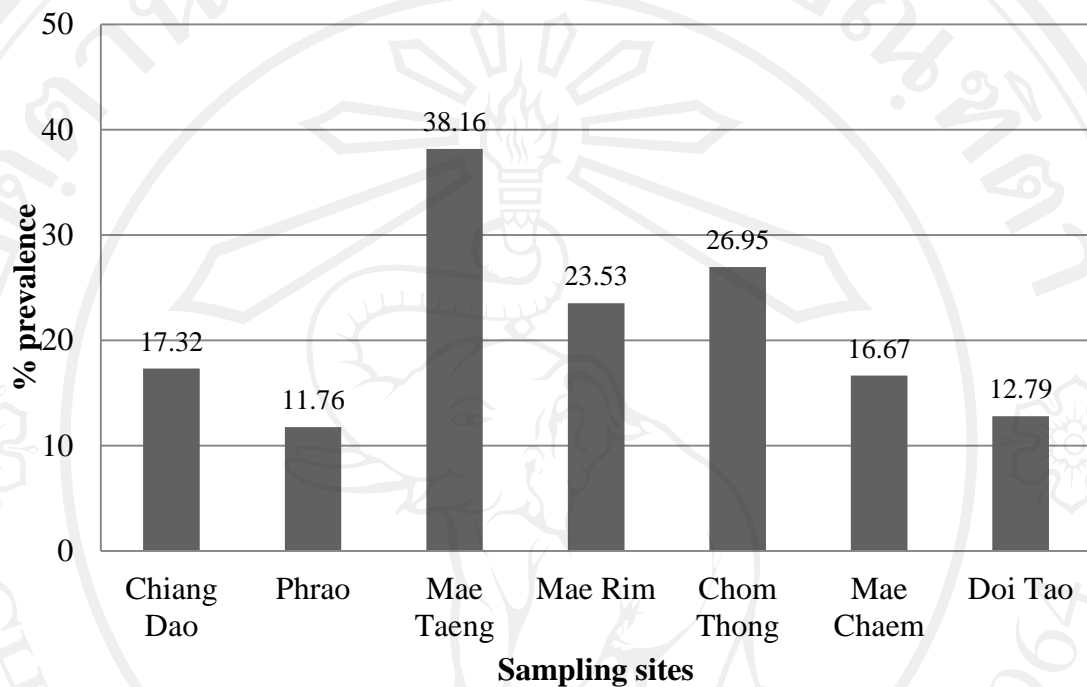


Figure 4.4 The total prevalence of cercariae infection of snails found in each sampling sites

The prevalence of infection were also high recorded in parapleurolophocercous cercaria (8.65%), followed by distome cercaria (5.88%) and monostome cercaria (5.19%), respectively. The xiphidiocercaria was shown lowest prevalence, with 0.35% (Fig. 4.5).

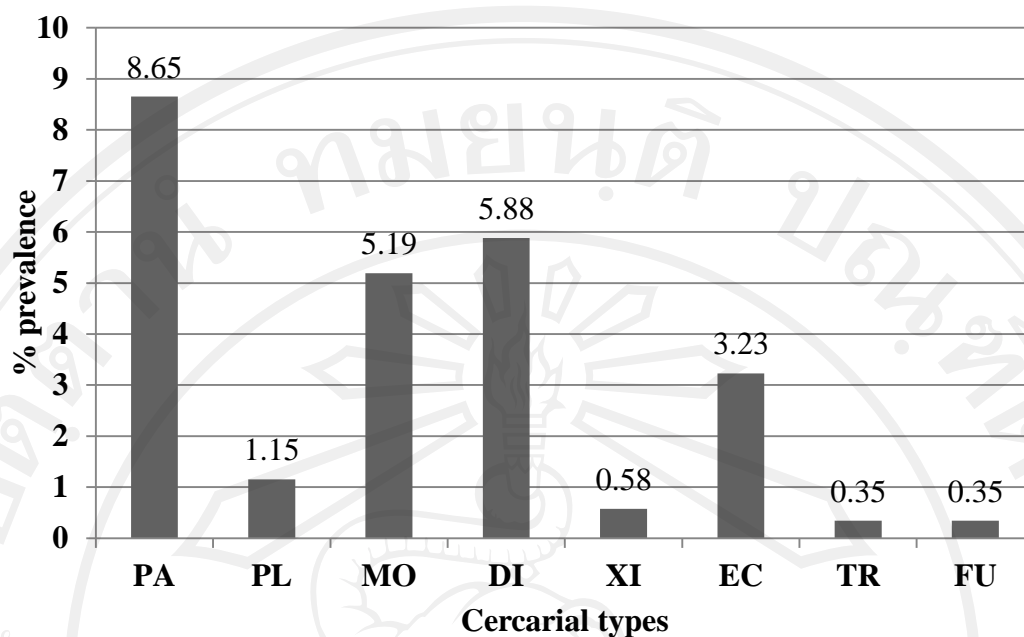


Figure 4.5 The prevalence of infection in each cercarial type found in snails. parapleurolophocercous cercaria (PA), pleurolophocercous cercaria (PL), monostome cercaria (MO), distome cercaria (DI), xiphidiocercaria (XI), echinostome cercaria (EC), transversotremacercaria (TR), furcocercous cercaria (FU)

The high infection of cercaria was found in 3 snails as followed *Bithynia siamensis* was found monostome cercaria (60.81%), *F. dorliaris* was found echinostome cercaria (58.97%), and *Brotia baccata* was found distome cercaria (58.06%). No infection of cercaria was found in 8 species of snails as *Brotia costula costula*, *Brotia citrina*, *F. polygamma*, *L. auricularia rubiginosa*, *M. jugicostis*, *Physa acuta* and *Thiara scabra*. In addition, mixed-infection of cecariae in snails was found 3 species of snails as *Tarebia granifera*, *M. tuberculata* and *F. martensi martensi*. *Tarebia granifera* was found 5 cercarial types as xiphidiocercaria, transversotremacercaria, distome cercaria, parapleurolophocercous cercaria and pleurolophocercous cercaria, in *M. tuberculata* found mixed-infection of cercaria in 3 types as distome cercaria, parapleurolophocercous cercaria and pleurolophocercous cercaria, *F. martensi martensi* found 2 types as furcocercous cercaria and echinostome cercaria (Table 4.1).

Table 4.1 The cercarial types and prevalence of infection found in snails

No.	Species	No. snails	Cercarial types	Prevalence (%)
1	<i>Bithynia siamensis</i>	74	monostome cercaria	60.81
2	<i>Brotia costula costula</i>	26	-	-
3	<i>Brotia citrina</i>	5	-	-
4	<i>Brotia baccata</i>	31	distome cercaria	58.06
5	<i>Eyriesia eyriesi</i>	52	-	-
6	<i>Filopaludina martensi</i>	62	furcocercous cercaria	4.84
	<i>martensi</i>		echinostome cercaria	8.06
7	<i>Filopaludina dorliaris</i>	39	echinostome cercaria	58.97
8	<i>Filopaludina polygamma</i>	4	-	-
9	<i>Lymnaea auricularia</i>	27	-	-
	<i>rubiginosa</i>			
10	<i>Melanoides tuberculata</i>	101	pleurolophocercous cercaria	5.94
			Parapleurolophocercous cercaria	15.84
			distome cercaria	19.80
11	<i>Melanoides jugicostis</i>	27	-	-
12	<i>Physa acuta</i>	117	-	-
13	<i>Tarebia granifera</i>	272	pleurolophocercous cercaria	1.47
			parapleurolophocercous cercaria	21.32
			xiphidiocercaria	1.84
			distome cercaria	1.47
			tranversotremacercaria	1.10
14	<i>Thiara scabra</i>	30	-	-
Total		867	8	25.26

4.4 *F. gigantea* life history study

4.4.1 Morphological study of *F. gigantea* larval stages

1) Eggs

The eggs are large, oval, yellowish-brown with a thin shell, and are flat and with operculated. They are 0.12-0.18 (0.15) mm in length and 0.08-0.11 (0.09) mm in width. Using the SEM study of eggs, the outer surface was described as smooth (Figs. 4.6-4.7).

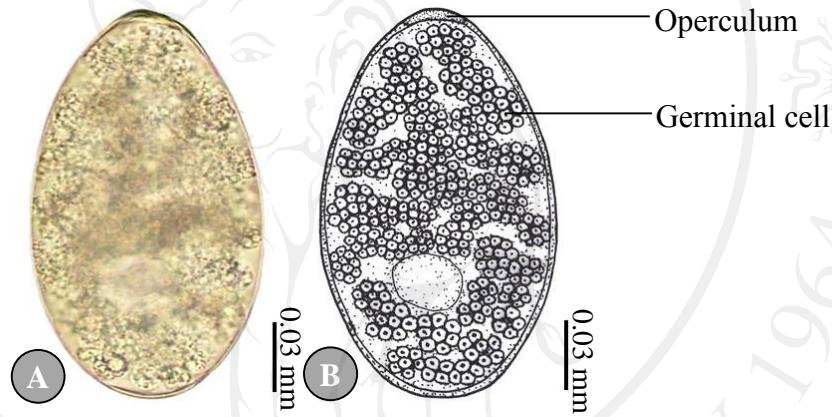


Figure 4.6 Illustration demonstrated the morphology of *F. gigantea* eggs; (A) photograph, (B) drawing

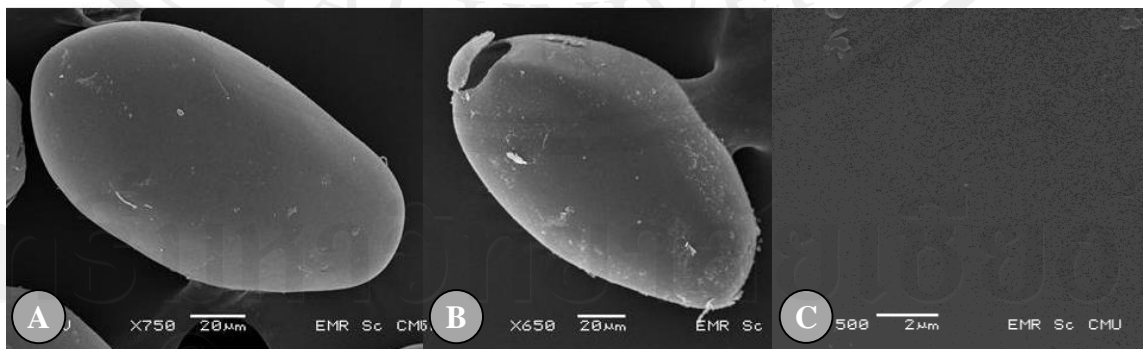


Figure 4.7 SEM photographs demonstrated the morphology of *F. gigantea* eggs; (A) showing the whole egg, (B) operculum of egg, (C) the smoothly surface of egg

2) Miracidium

The body is elongated and conical, and it has a broad anterior and a posterior that tapers to a blunt end. The body is 0.13-0.17 (0.15) mm in length and 0.05-0.09 (0.07) mm in width. The surface is completely occupied with cilia. The apical papilla is shown in the middle of the anterior part and there is a pair of darkly stained eye-spots that are visible near the anterior part of the body. Germinal cells are scattered at the posterior segment (Figs. 4.8-4.9).

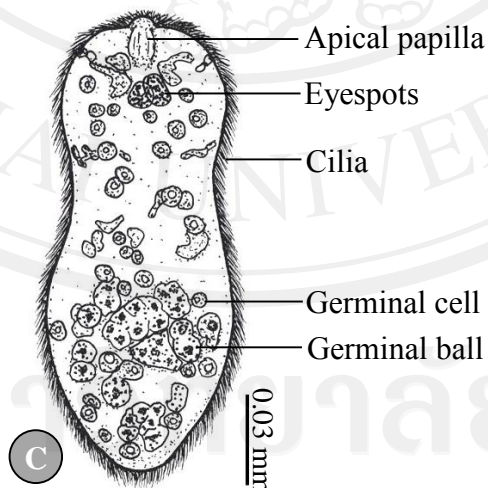
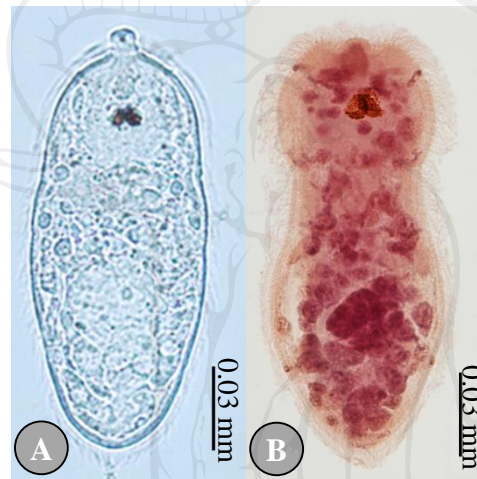


Figure 4.8 Illustration demonstrated the morphology of *F. gigantea* miracidium; (A) photographs of living miracidium, (B) permanent slide, (C) drawing

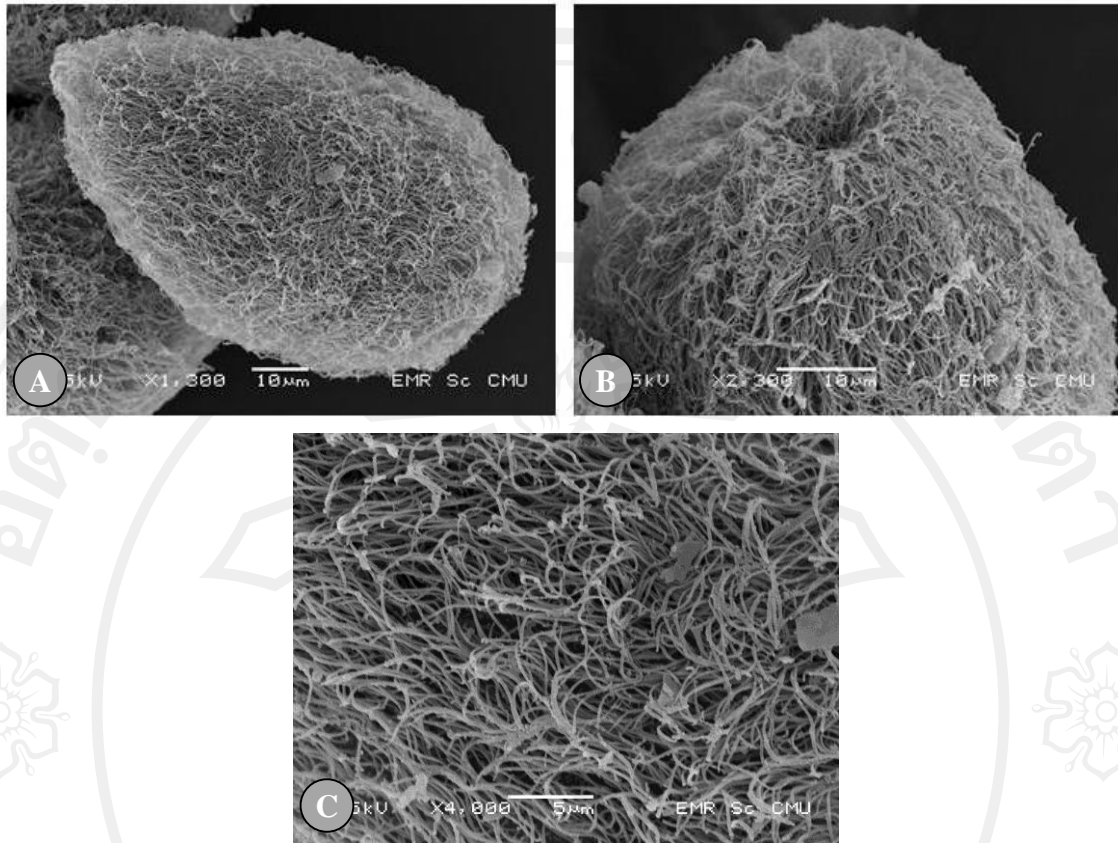


Figure 4.9 SEM photographs demonstrated the morphology of *F. gigantea* miracidium; (A) showing the conical body shape and completely covered with cilia, (B) the open of apical papilla, (C) the enlargement of cilia

3) Sporocyst

The young sporocyst is oval shaped, 0.11-0.15 (0.13) mm in length and 0.10-0.11 (0.10) mm in width. The sporocyst consisted initially of a minute ball of tightly packed germinal cells. At this stage, the eyespots can be seen. Each germinal cell gives rise to new germinal cells and these then multiplies to become germinal balls. After that, the bodies of the mature sporocyst are elongated and formed to the redia (Figs. 4.10-4.11).

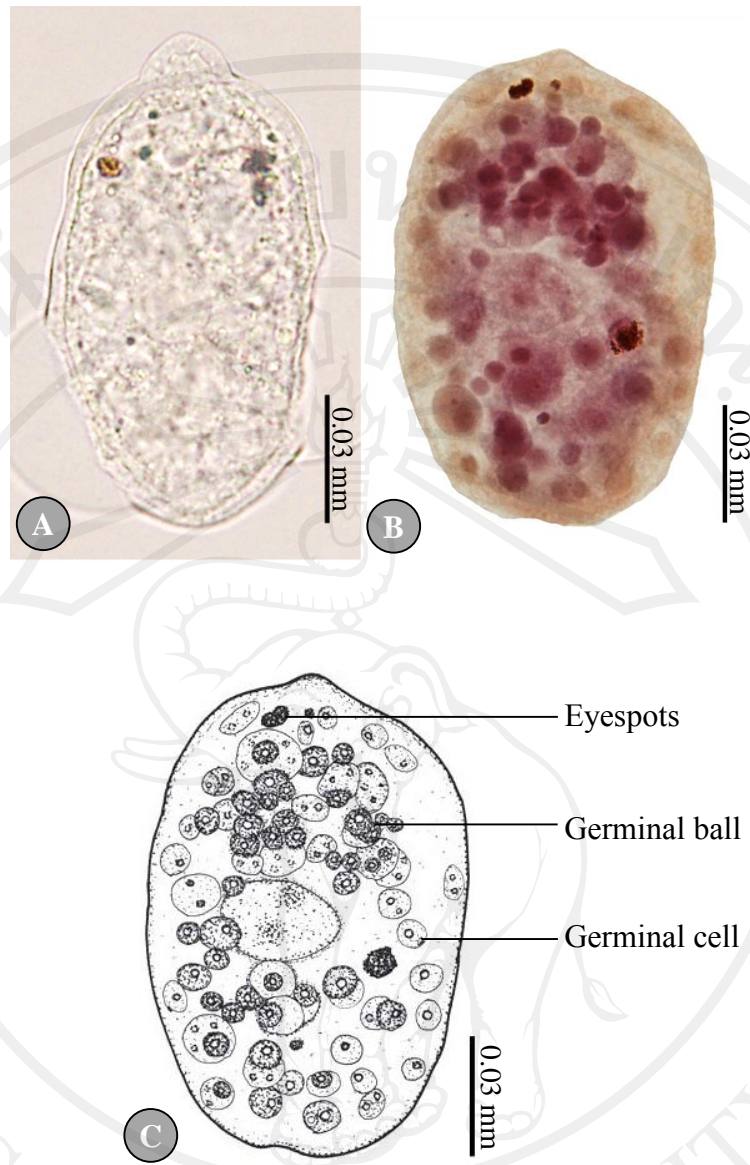


Figure 4.10 Illustration demonstrated the morphology of *F. gigantea* young sporocyst; (A) photographs of living sporocyst, (B) permanent slide, (C) drawing

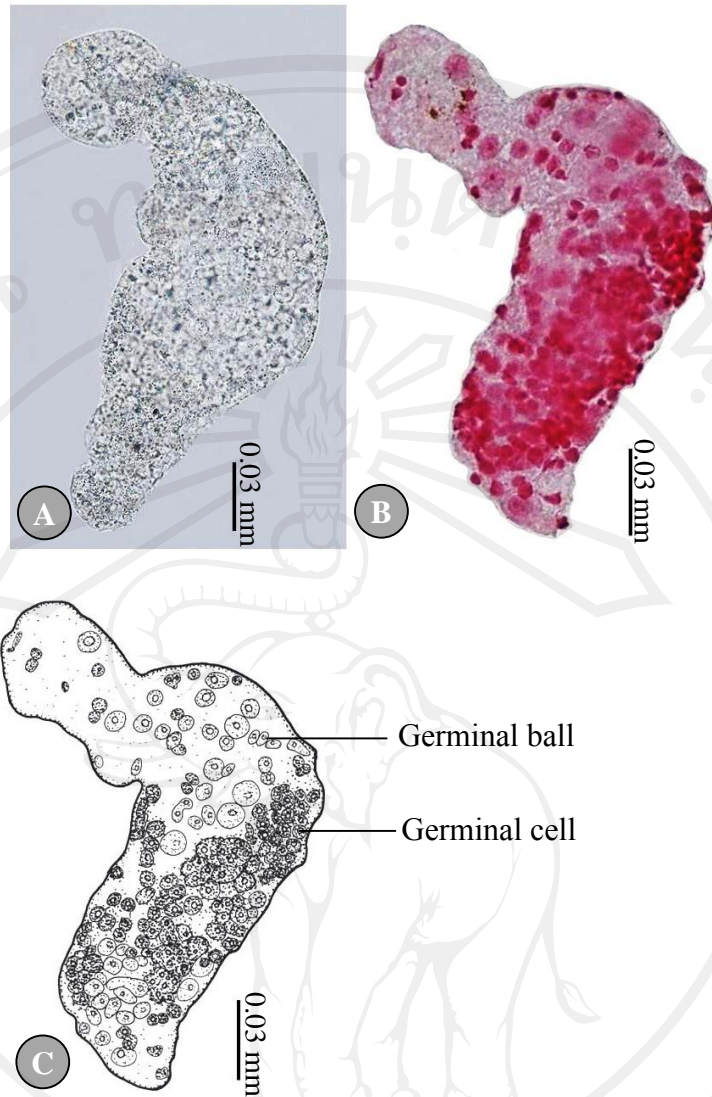


Figure 4.11 Illustration demonstrated the morphology of *F. gigantea* mature sporocyst that elongated and formed with redia; (A) photographs of living mature sporocyst, (B) permanent slide, (C) drawing

4) Redia

The rediae are roughly cylindrical in shape and the birth pore is located at the anterior end. The unique characteristics of this stage include two lateral projections at the posterior end and the primitive gut is presented. The redia stage consists of a mother redia and a daughter

redia. The mother rediae contain many daughter rediae and germinal balls (Fig. 4.12), while the daughter rediae contain many cercariae and germinal balls (Fig. 4.13).

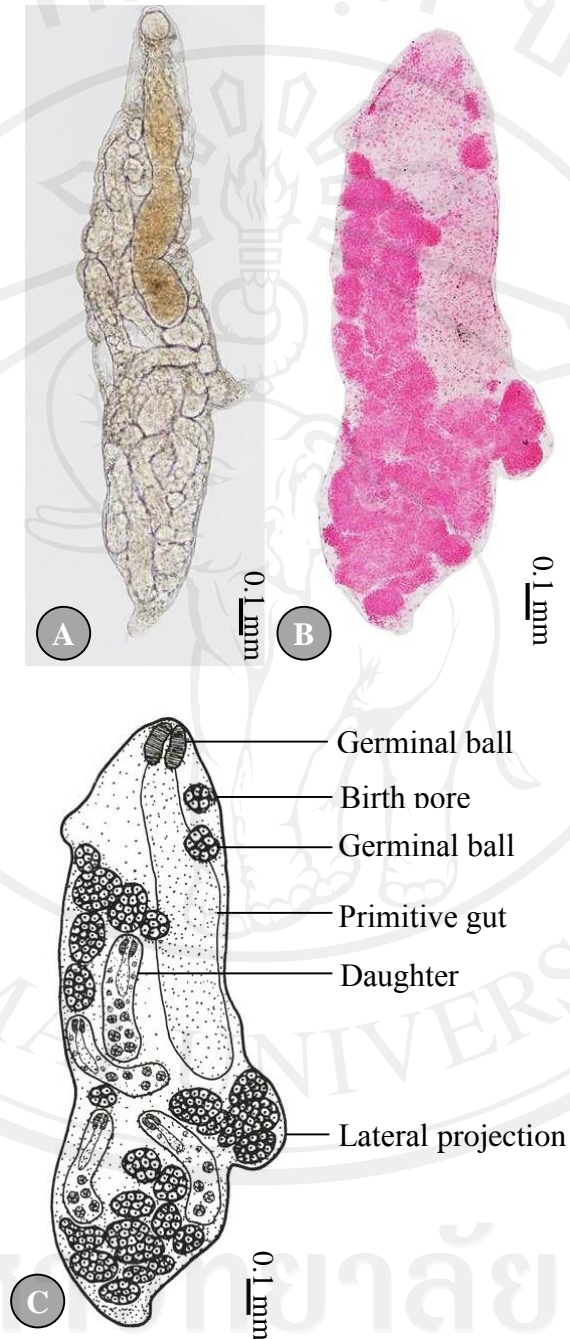


Figure 4.12 Illustration demonstrated the morphology of *F. gigantica* mother redia containing with daughter rediae; (A) photographs of living mother redia, (B) permanent slide, (C) drawing

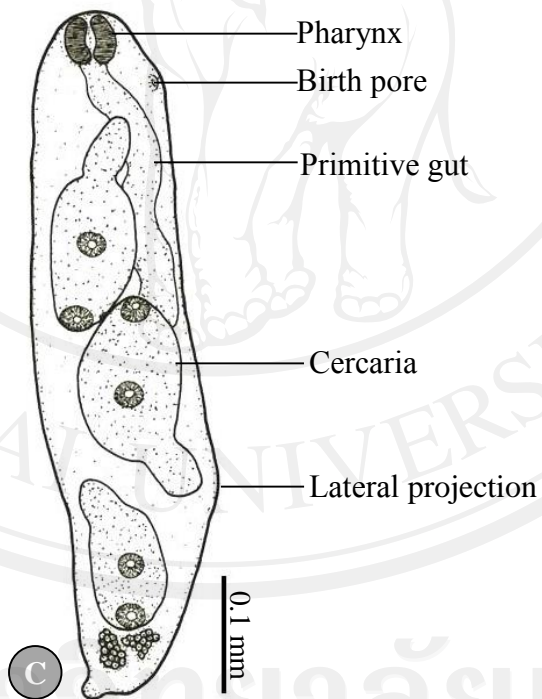
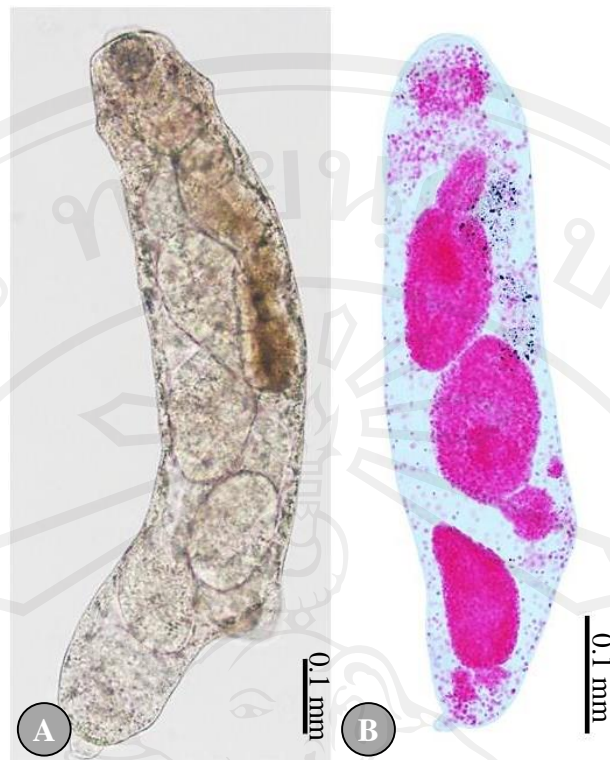


Figure 4.13 Illustration demonstrated the morphology of *F. gigantica* daughter redia containing with cercaria; (A) photographs of living daughter, (B) redia permanent slide, (C) drawing

5) Cercaria

The type of cercaria was generated as gymnocephalus cercaria, with tadpole-like shape. The body is a discoid shape and with a long tail. They possess an oral sucker and a ventral sucker in the center of their bodies and have very conspicuous cystogenous glands and a forked intestine. Both a pharynx and prepharynx are present (Figs. 4.14-4.15).



Figure 4.14 Illustration demonstrated morphology of *F. gigantica* cercaria (gymnocephalus cercaria); (A) photographs of living cercaria, (B) permanent slide

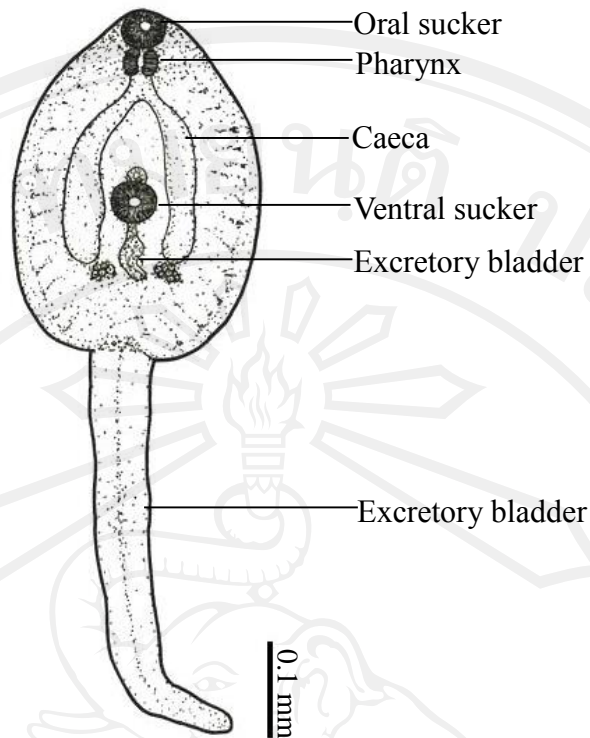


Figure 4.15 Illustration demonstrated the drawing morphology of *F. gigantica* cercaria (gymnocephalus cercaria)

6) Metacercaria

The metacercariae of *F. gigantica* are covered with capsules, which serve as protection from environmental impacts. The diameters of the capsules range from 0.26 to 0.30 (0.28) mm (Fig. 4.16). The metacercariae has a double thick wall that consists of an outer and inner cyst, which is 0.19-0.23 (0.20) mm in diameter. The cyst is white when laid, and is almost immediately infective to the definitive host. After a day or two the cyst gradually becomes yellow and darkens in color (Fig. 4.17).

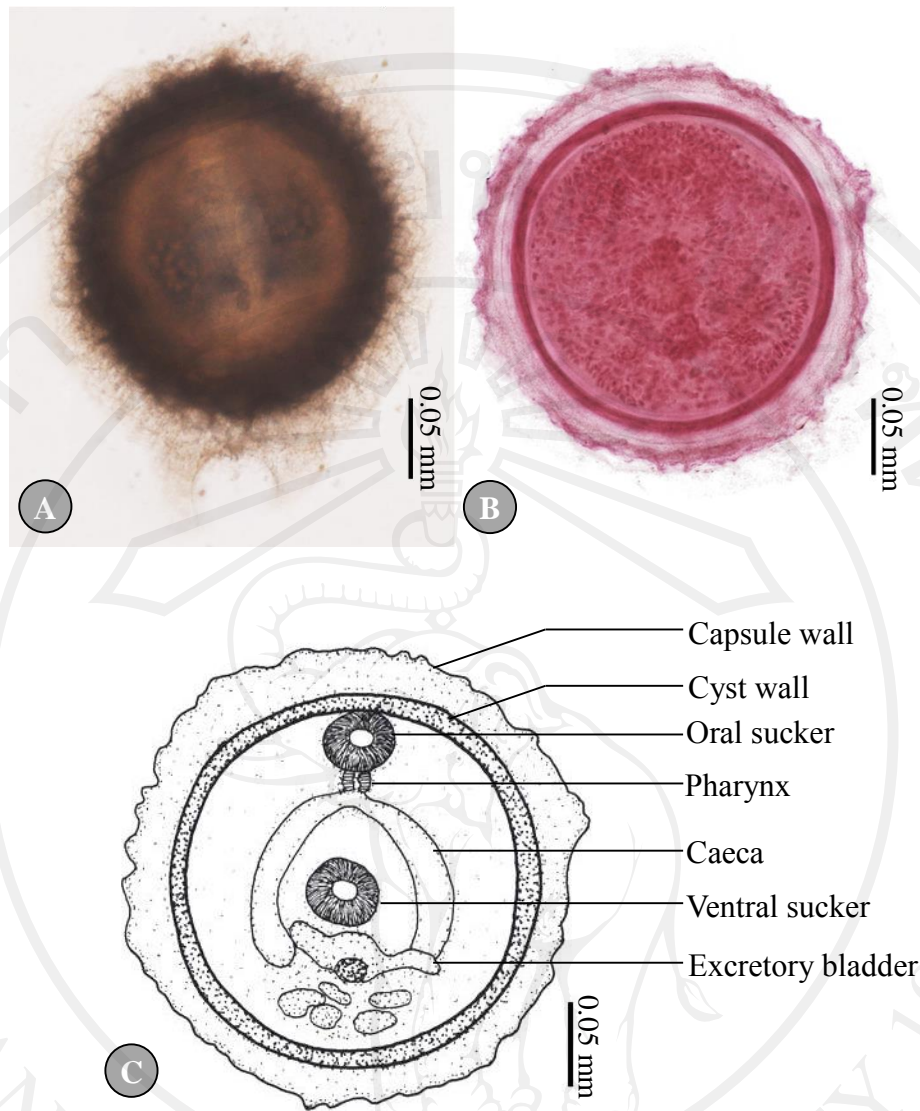


Figure 4.16 Illustration demonstrated the morphology of capsule of metacercaria; (A) photographs of living capsules, (B) permanent slide, (C) drawing

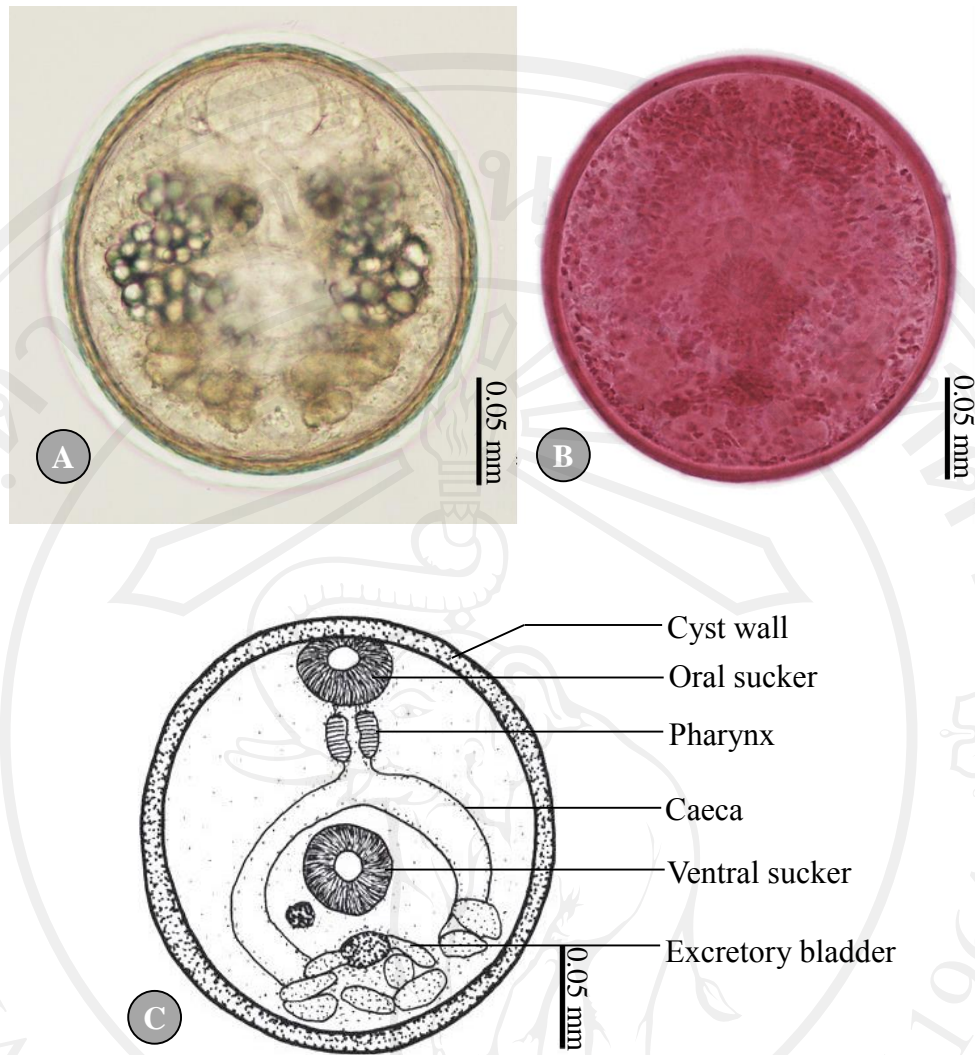


Figure 4.17 Illustration demonstrated the morphology of metacercaria; (A) photographs of living metacercaria, (B) permanent slide, (C) drawing

4.4.2 Hatching of miracidium from eggs

After incubation, the eggs developed from the unembryonate stage (Fig. 4.18a) to the embryonated stage (Fig. 4.18b) on day 3, and they then fully developed to miracidium eggs (Fig. 4.18c). Hatching began to occur on day 11, post incubation, while most eggs had hatched on day 12, post incubation. Fully-developed miracidium then protruded from the eggs by pushing through the operculum of the eggs (Fig. 4.18d).



Figure 4.18 Photographs demonstrated the different stages of eggs during the incubation period; (A) unembryonated egg, (B) embryonated egg, (C) fully miracidium egg, (D) escaping miracidium

4.4.3 Infection of miracidium in snails

Free-swimming larval miracidium then encountered and penetrated the appropriate snail as an intermediate host (*L. auricularia rubiginosa*). Miracidium then attached themselves to the snails' body via the apical papilla and then lost its ciliated covering and transformed to the next stage. For those miracidium failing to find a snail host, generally they died within 24 hours. The snail that was infected then presented the miracidium, which transformed to the next three larval stages, referred to as: sporocyst, redia, and cercaria. The developmental stages in the experimental snails are depicted in figure 4.19.

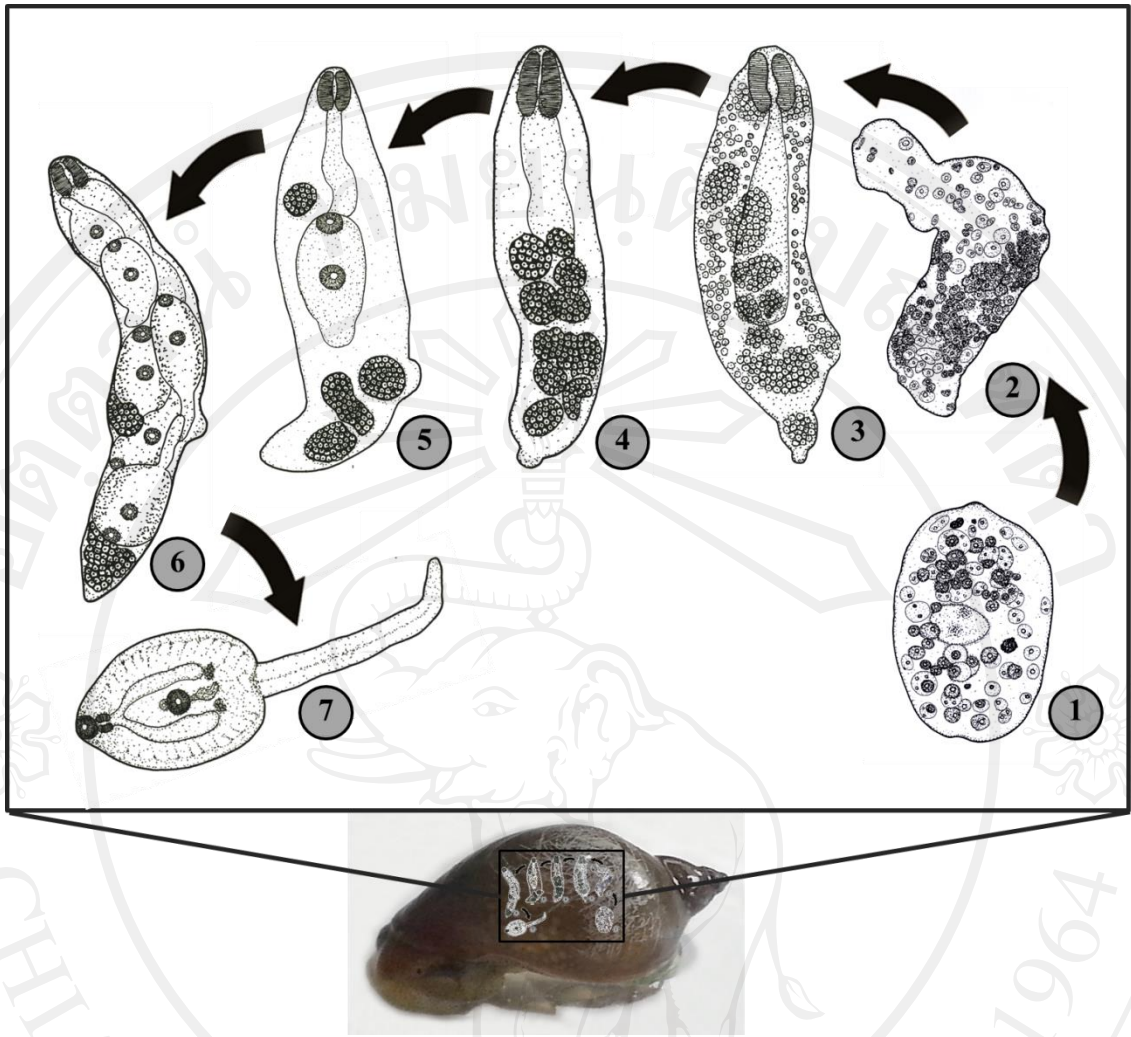


Figure 4.19 Illustration demonstrated the development of the larval stages, as found in experimental snail hosts, *Lymnaea auricularia rubiginosa*

Figure 4.19 reveals the developmental stage of *F. gigantica* in the experimental snail host, *L. auricularia rubiginosa*. The miracidium then loses its ciliated covering and becomes a young sporocyst on day 3 PI. Young sporocyst consisting of packed germinal cells and eyespots can now be seen at this stage (1). On day 7 PI, the young sporocyst transformed to become mature sporocyst, which are redia-like shaped, but no pharynx or primitive gut (2) are present. On day 10 PI, the mature sporocyst transformed to become young mother redia, with the visible pharynx and primitive gut, which are the unique characteristics of the redia (3). Each germinal cell in the

sporocyst developed and formed the germinal ball on day 14 PI (4). Young daughter redia and cercaria were present on day 21 PI (5). On day 24 PI, the daughter redia and young cercaria became fully developed (6), and then the fully developed cercariae were separated from the redia through a birth pore to the snail's tissue and were then shed from the snails to the body of water on day 39 PI (7).

4.4.4 Encystation of metacercaria on rice plants

The active cercariae emerged from the snail and swam freely to search for the substrate for the encystment stage. Then cercariae then came into contact with a rice plant or other substrate, the free-swimming cercaria simultaneously adhered to the plant, released the outer layer of the cyst and produced capsules to cover their bodies. At this point, the cercariae then lost its tail during the metacercarial stage (Fig. 4.20-4.21). Life cycle will be complete when the metacercariae were eaten by a definitive host, such as a mammal.

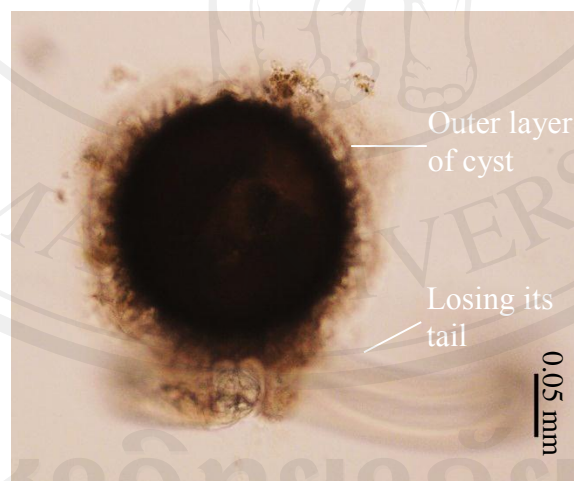


Figure 4.20 Photographs demonstrated the cercariae released outer layer of the cyst and lost its tail

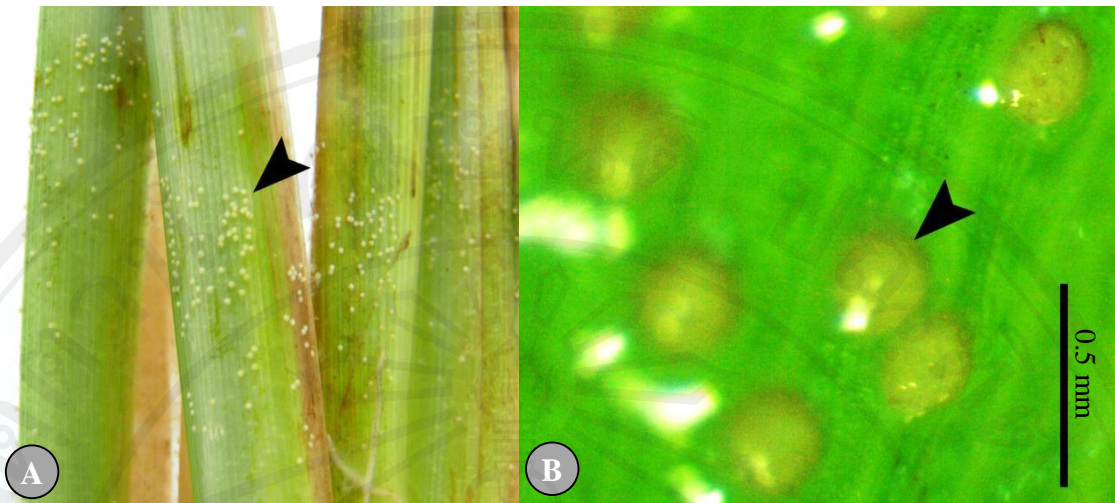


Figure 4.21 Photographs demonstrated the capsule of metacercaria (arrowhead); (A) they were adhered to the stem of the rice plant, (B) the enlargement of capsule of metacercaria

4.4.5 Incidences and worm recovery rate in experimental hosts

The metacercariae were experimentally confirmed by successful development of adult worms in experimental hosts; dwarf hamsters and albino mice. Thirty encysted metacercariae were experimental force fed to albino mice and dwarf hamsters. The metacercariae were excysted to young adult worms and were then recovered in the intestine of both experimental hosts on day 3 and day 6 PI (post- infection), until day 9 PI, when they were found in the liver of the host (Table 4.3)

The rates of parasitic incidence of both experimental hosts were 100%. Average worm recovery rates were 35.83% (172/480) and 36.00% (162/450) in albino mice and dwarf hamsters, respectively. The worm recovery rates of both experimental hosts were continuously decreased until the end of experimental infection. The dwarf hamsters were died on day 45 PI, as a

result of having their liver destroyed by the migration and penetration of the worms (Fig. 4.22), while albino mice still alive in day 48 PI. The highest worm recovery rates of albino mice were 63.33% at day 15 PI, while dwarf hamster were 53.33% at day 3 and 9 PI, respectively. (Fig. 4.23; Table 4.2).

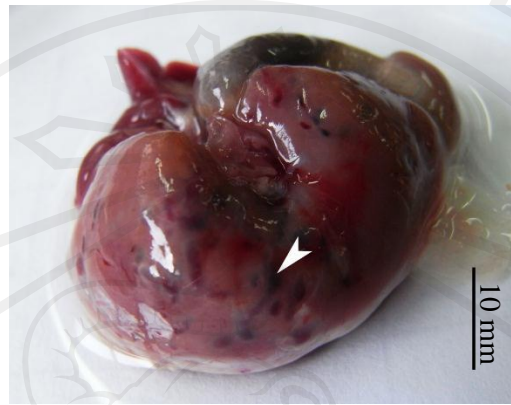


Figure 4.22 Infected liver of a dwarf hamster was severely destroyed due to migration and penetration of worms (arrow head)

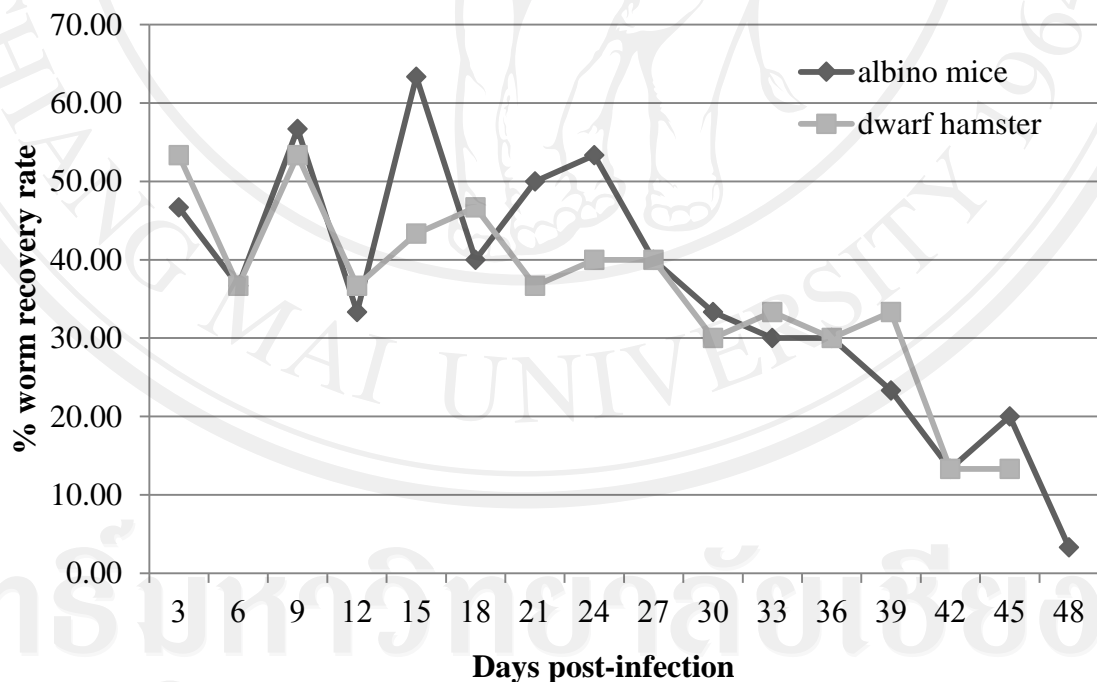


Figure 4.23 The worm recovery rates of *F. gigantica* adult worms in albino mice and dwarf hamsters were sacrificed every 3 day PI

Table 4.2 The worm recovery rates of *F. gigantica* adult worms in albino mice and dwarf hamsters

Day PI	No. metacercaria	Dwarf hamster			Albino mice		
		No. worms	Site of infection	Worm recovery (%)	No. worms	Site of infection	Worm recovery (%)
3	30	16	intestine	53.33	14	intestine	46.67
6	30	11	intestine	36.67	11	intestine	36.67
9	30	16	liver	53.33	17	liver	56.67
12	30	11	liver	36.67	10	liver	33.33
15	30	13	liver	43.33	19	liver	63.33
18	30	14	liver	46.67	12	liver	40.00
21	30	11	liver	36.67	15	liver	50.00
24	30	12	liver	40.00	16	liver	53.33
27	30	12	liver	40.00	12	liver	40.00
30	30	9	liver	30.00	10	liver	33.33
33	30	10	liver	33.33	9	liver	30.00
36	30	9	liver	30.00	9	liver	30.00
39	30	10	liver	33.33	7	liver	23.33
42	30	4	liver	13.33	4	liver	13.33
45	30	4	liver	13.33	6	liver	20.00
48	30	-	-	-	1	liver	3.33
Av g.	480	162		36.00	172		35.83

4.4.6 Maturation of adult worms in experimental definitive host; albino mice and dwarf hamsters

The development patterns of *F. gigantica* both hosts were shown that the sizes of body width, body length, oral and ventral sucker of *F. gigantica* in both hosts were continuously increased. The genital pore was initially recovered on day 9 PI, while caeca found on day 18 PI. But, testes and ovary

were discovered in day 27 PI and developed maturely in day 39 PI. Immature eggs (Fig. 4.24) were discovered in day 42 PI, indicated that parasites begin to mature.

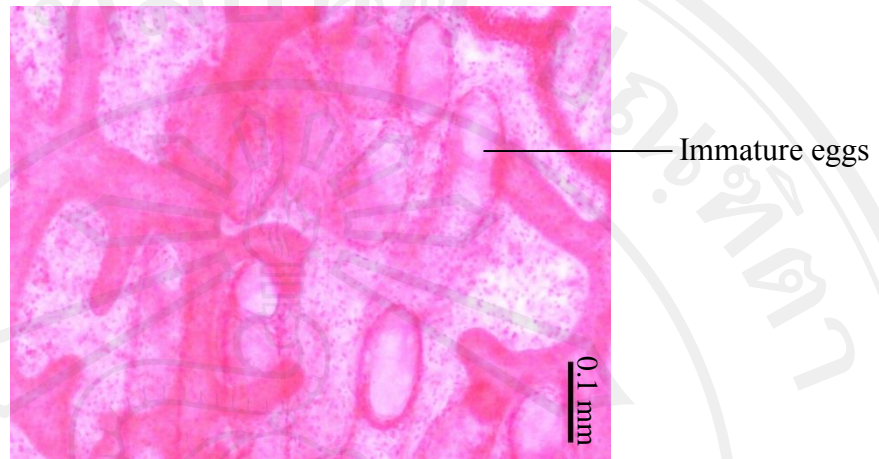


Figure 4.24 Immature eggs were discovered in day 42 PI on uterus of dwarf hamsters

The pattern of *F. gigantica* development in both hosts was depicted in figure 4.25-4.26. The minimum and maximum sizes of body of *F. gigantica* found in dwarf hamster were 0.24 x 0.42 mm (day 3 PI) and 3.80 x 13.90 mm (day 45 PI) (Table 4.3). While, the minimum and maximum sizes of body in albino mice were 0.19 x 0.0.23 mm (day 3 PI) and 2.85 x 14.68 mm (day 48 PI) (Table 4.3). The development of organ was similarity with dwarf hamsters as the genital pore was initially recovered on day 9 PI, while caeca found on day18 PI. But, testes and ovary were discovered in day 27 PI and developed maturely in day 39 PI. Immature eggs were discovered in day 42 PI and these eggs were developed maturely in day 48 PI, indicated that parasites maturation. Therefore, it can be confirmed that *F. gigantica* metacercariae derived from experimental encystment could be infected and developed in both hosts as well.

Table 4.3 Average measurements (mm) of young to mature adult of *F. gigantica* in both experimental hosts; albino mice and dwarf hamsters

Days of PI	No. of worms	Body		Oral sucker		Ventral sucker	
		width	length	width	length	width	length
Hamsters							
3	4	0.24	0.42	0.07	0.06	0.06	0.07
6	3	0.32	0.72	0.10	0.09	0.13	0.12
9	11	0.47	1.14	0.13	0.11	0.17	0.15
12	3	0.48	1.27	0.14	0.13	0.19	0.17
15	5	0.72	2.11	0.22	0.18	0.29	0.27
18	6	0.97	1.35	0.27	0.24	0.35	0.33
21	6	0.97	1.35	0.34	0.25	0.38	0.37
24	6	0.97	1.35	0.39	0.32	0.55	0.51
27	5	1.42	5.60	0.46	0.35	0.52	0.52
30	7	1.61	5.52	0.53	0.41	0.62	0.63
33	9	2.45	7.04	0.51	0.46	0.72	0.71
36	7	2.46	8.54	0.54	0.46	0.83	0.82
39	9	2.98	9.56	0.55	0.46	0.79	0.77
42	3	2.73	9.62	0.53	0.50	0.74	0.77
45	2	3.80	13.90	0.56	0.45	0.89	0.92
Albino mice							
3	3	0.19	0.23	0.07	0.05	0.06	0.07
6	5	0.27	0.68	0.09	0.06	0.10	0.10
9	6	0.36	0.81	0.10	0.09	0.17	0.20
12	4	0.54	1.38	0.14	0.11	0.18	0.19
15	9	0.78	2.16	0.24	0.18	0.31	0.26
18	7	0.87	2.63	0.27	0.20	0.35	0.32
21	4	1.27	4.21	0.35	0.30	0.44	0.45
24	4	1.51	4.13	0.42	0.30	0.47	0.47
27	6	1.75	5.91	0.43	0.33	0.57	0.53
30	7	2.18	7.26	0.47	0.39	0.66	0.61
33	6	2.25	7.91	0.48	0.42	0.70	0.69
36	6	2.76	8.78	0.53	0.44	0.70	0.67
39	6	2.83	10.75	0.54	0.44	0.74	0.76
42	3	3.69	12.60	0.57	0.51	0.82	0.82
45	2	2.48	12.21	0.43	0.44	0.64	0.69
48	1	2.85	14.68	0.50	0.42	0.82	0.77

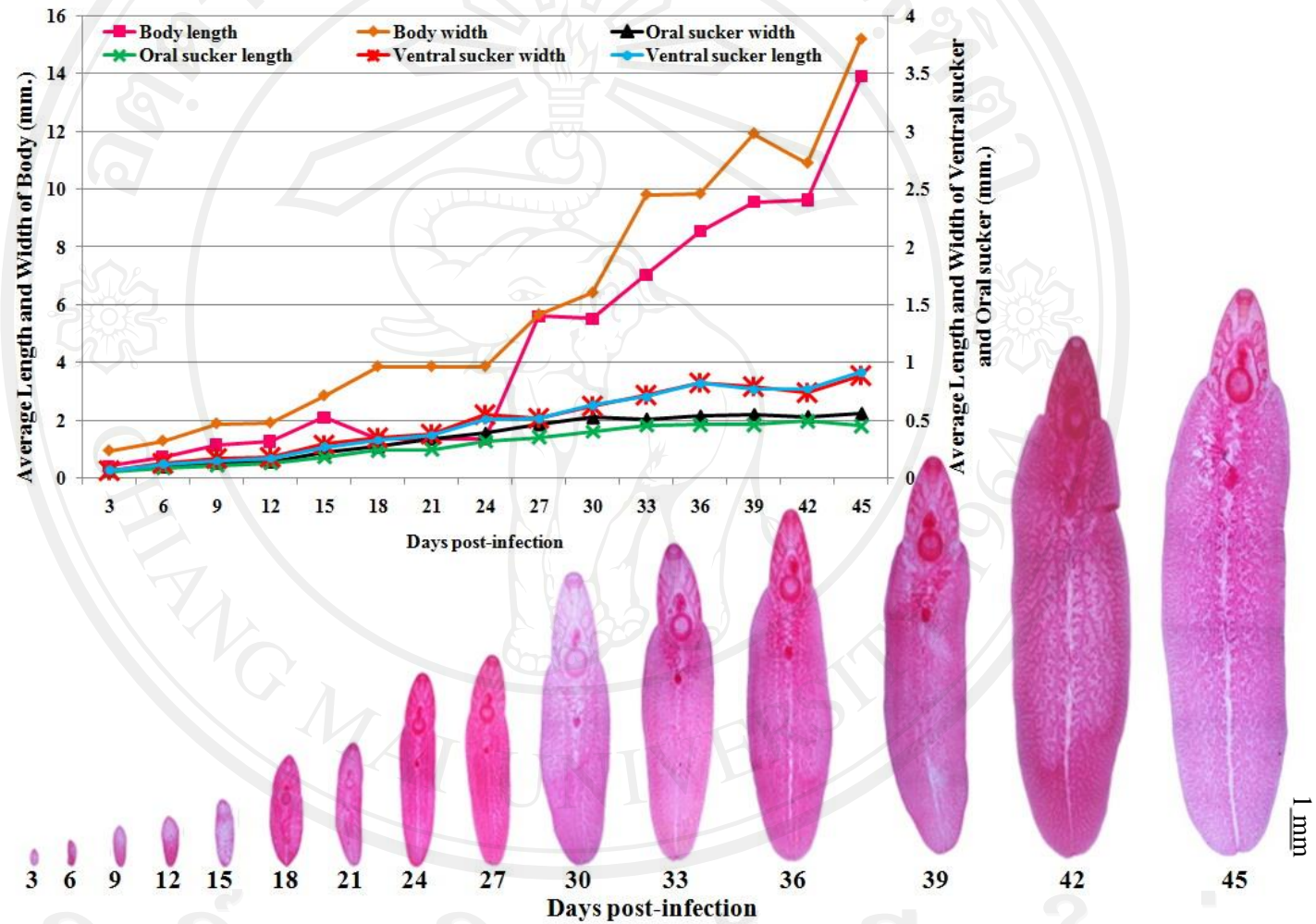


Figure 4.25 Changes of morphological and average measurements of *F. gigantica* recovered from dwarf hamsters

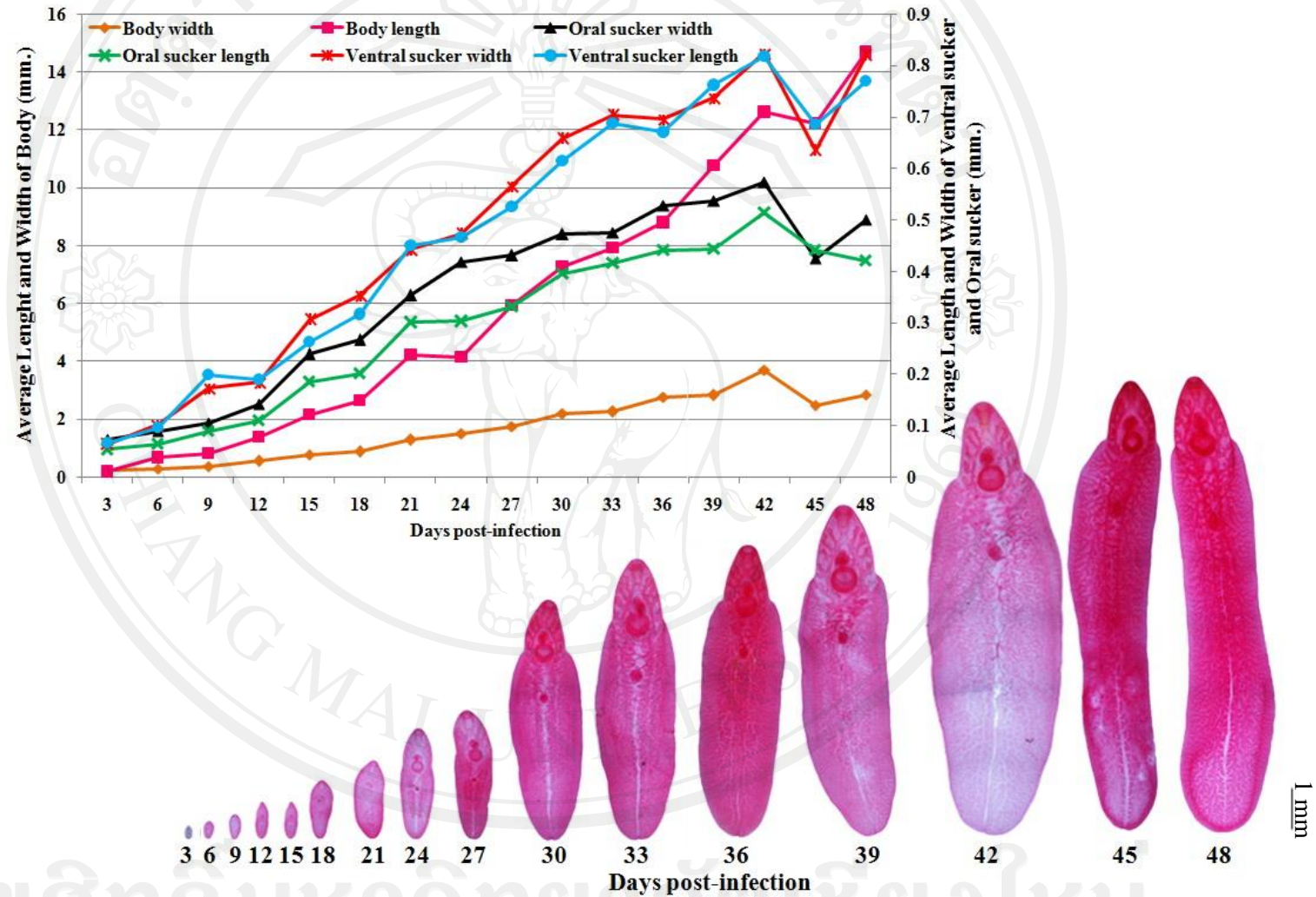


Figure 4.26 Changes of morphological and average measurements of *F. gigantica* recovered from albino mice

4.5 Molecular biological study

4.5.1 Development of specific primer

1) HAT-RAPD PCR

Genomic DNA of *F. gigantica* was compared with genomic DNA of related-species trematodes as: *Haplorchis taichui*, *Stellantchasmus* sp., *Opisthorchis viverrini*, *Haplorchoides* sp., *Fischoederius elongatus*, *Orthocoelium streptocoelium*, *Paramphistomum epiclitum*, *Posthodiplostomum* sp., *Ganeo tigrinus*, and *Clinostomum philippinensis* (Appendix B).

Sixteen commercially random arbitrary primers as OPA-01, OPA-02, OPA-03, OPA-04, OPA-09, OPA-10, OPN-02, OPN-03, OPN-04, OPN-05, OPN-06, OPN-07, OPN-08, OPN-09, OPN-10, and OPP-11 were used individually for HAT-RAPD PCR, and the reaction was carried out in a final volume of 20 μ l, with common PCR composition. The reactions were performed in a LifePro Thermal Cycler (Bioer Serves Life ,USA) and the PCR conditions were as follows: 1 cycle of 95 °C for 2 minutes, 35 cycles of 95 °C for 45 seconds, 48 °C for 45 seconds, 72 °C for 1 minutes and 1 cycle of final extension at 72 °C for 7 minutes. HAT-RAPD PCR products were separated on 1.4% TBE agarose gel electrophoresis, stained with ethidium bromide, and photographed by a Kodak digital camera (Gel Logic 100). The HAT-RAPD profiles of all trematodes generated from each primer including number of bands were sequentially depicted in figure 4.27-4.42 and table 4.4-4.19.

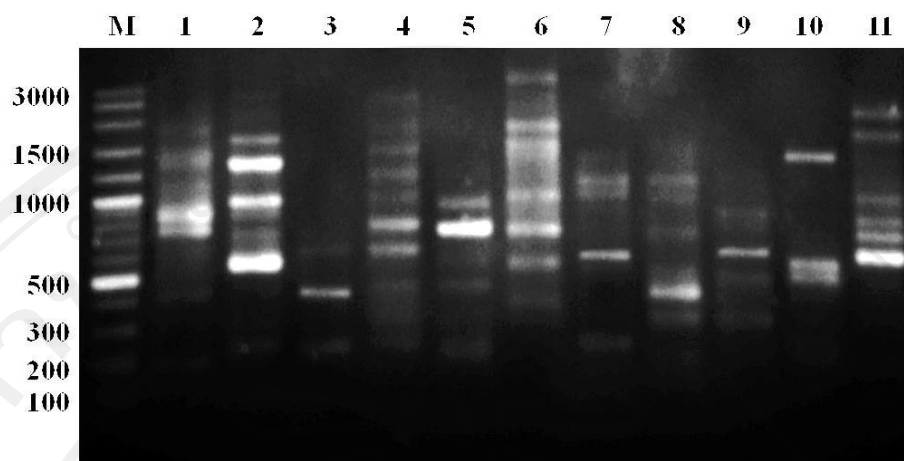


Figure 4.27 HAT-RAPD profiles generated by OPA-01 primer

Lane M: 100 bp DNA marker, lane 1: *Fasciola gigantica*, lane 2: *Paramphistomum epiclitum*, lane 3: *Fischoederius elongatus*, lane 4: *Orthocoelium streptocoelium*, lane 5: *Haplorchis taichui*, lane 6: *Stellantchasmus* sp., lane 7: *Haplorchoides* sp., lane 8: *Opisthorchis viverrini*, lane 9: *Ganeo tigrinus*, lane 10: *Clinostomum philippinensis*, lane 11: *Posthodiplostomum* sp.

Table 4.4 Number of fragment generated and fragment size ranged of each trematode samples based on HAT-RAPD profiles of OPA-01 primer

Lane	Trematodes	No. fragments	Size ranged (bp)
1	<i>Fasciola gigantica</i>	3	750-1400
2	<i>Paramphistomum epiclitum</i>	4	600-1800
3	<i>Fischoederius elongatus</i>	3	250-600
4	<i>Orthocoelium streptocoelium</i>	8	250-2500
5	<i>Haplorchis taichui</i>	4	250-900
6	<i>Stellantchasmus</i> sp.	7	400-3000
7	<i>Haplorchoides</i> sp.	4	250-1200
8	<i>Opisthorchis viverrini</i>	5	300-1200
9	<i>Ganeo tigrinus</i>	3	280-900
10	<i>Clinostomum philippinensis</i>	3	400-1500
11	<i>Posthodiplostomum</i> sp.	6	600-2250

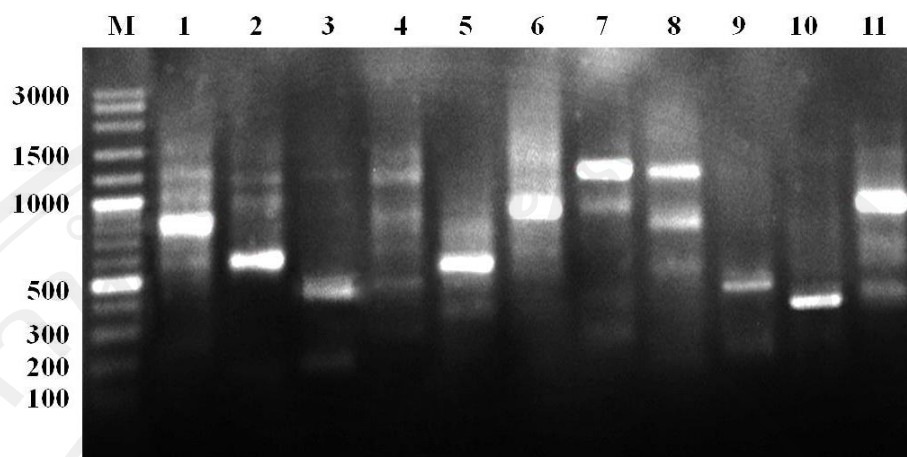


Figure 4.28 HAT-RAPD profiles generated by OPA-02 primer

Lane M: 100 bp DNA marker, lane 1: *Fasciola gigantica*, lane 2: *Paramphistomum epiclitum*, lane 3: *Fischoederius elongatus*, lane 4: *Orthocoelium streptocoelium*, lane 5: *Haplorchis taichui*, lane 6: *Stellantchasmus* sp., lane 7: *Haplorchoides* sp., lane 8: *Opisthorchis viverrini*, lane 9: *Ganeo tigrinus*, lane 10: *Clinostomum philippinensis*, lane 11: *Posthodiplostomum* sp.

Table 4.5 Number of fragment generated and fragment size ranged of each trematode samples based on HAT-RAPD profiles of OPA-02 primer

Lane	Trematodes	No. fragments	Size ranged (bp)
1	<i>Fasciola gigantica</i>	4	600-1300
2	<i>Paramphistomum epiclitum</i>	3	600-1200
3	<i>Fischoederius elongatus</i>	3	200-1200
4	<i>Orthocoelium streptocoelium</i>	6	300-1500
5	<i>Haplorchis taichui</i>	3	350-800
6	<i>Stellantchasmus</i> sp.	1	900
7	<i>Haplorchoides</i> sp.	3	300-1200
8	<i>Opisthorchis viverrini</i>	3	600-1200
9	<i>Ganeo tigrinus</i>	1	500
10	<i>Clinostomum philippinensis</i>	1	400
11	<i>Posthodiplostomum</i> sp.	3	400-1000

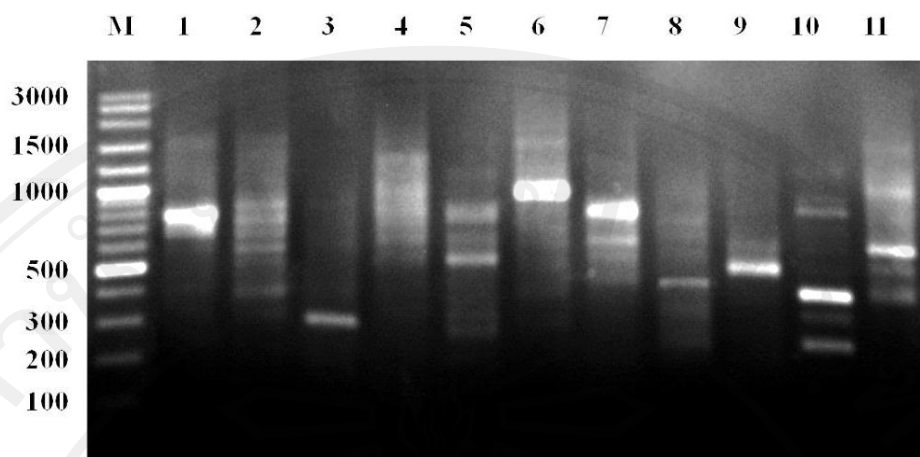


Figure 4.29 HAT-RAPD profiles generated by OPA-03 primer

Lane M: 100 bp DNA marker, lane 1: *Fasciola gigantica*, lane 2: *Paramphistomum epiclitum*, lane 3: *Fiscoederius elongatus*, lane 4: *Orthocoelium streptocoelium*, lane 5: *Haplorchis taichui*, lane 6: *Stellantchasmus* sp., lane 7: *Haplorchoides* sp., lane 8: *Opisthorchis viverrini*, lane 9: *Ganeo tigrinus*, lane 10: *Clinostomum philippinensis*, lane 11: *Posthodiplostomum* sp.

Table 4.6 Number of fragment generated and fragment size ranged of each trematode samples based on HAT-RAPD profiles of OPA-03 primer

Lane	Trematodes	No. fragments	Size ranged (bp)
1	<i>Fasciola gigantica</i>	1	750
2	<i>Paramphistomum epiclitum</i>	5	400-850
3	<i>Fiscoederius elongatus</i>	1	300
4	<i>Orthocoelium streptocoelium</i>	5	550-1250
5	<i>Haplorchis taichui</i>	3	550-800
6	<i>Stellantchasmus</i> sp.	1	1000
7	<i>Haplorchoides</i> sp.	3	450-800
8	<i>Opisthorchis viverrini</i>	1	400
9	<i>Ganeo tigrinus</i>	1	500
10	<i>Clinostomum philippinensis</i>	4	250-800
11	<i>Posthodiplostomum</i> sp.	4	400-1500

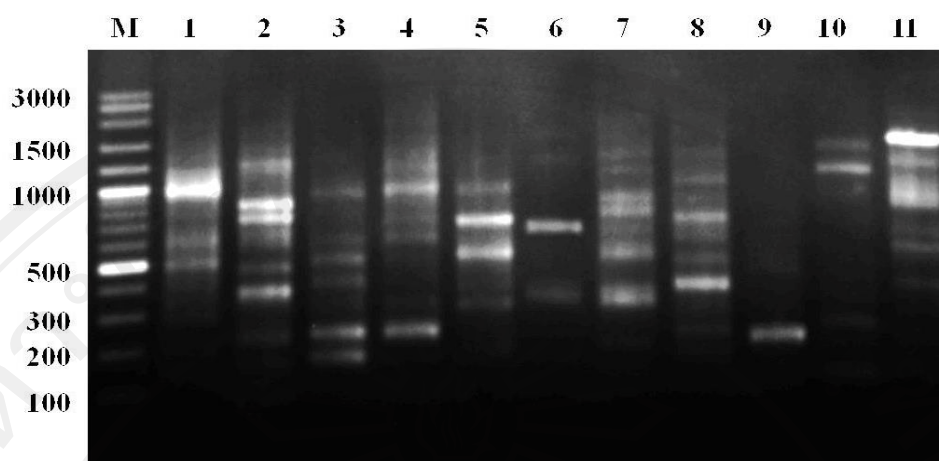


Figure 4.30 HAT-RAPD profiles generated by OPA-04 primer

Lane M: 100 bp DNA marker, lane 1: *Fasciola gigantica*, lane 2: *Paramphistomum epiclitum*, lane 3: *Fischoederius elongatus*, lane 4: *Orthocoelium streptocoelium*, lane 5: *Haplorchis taichui*, lane 6: *Stellantchasmus* sp., lane 7: *Haplorchoides* sp., lane 8: *Opisthorchis viverrini*, lane 9: *Ganeo tigrinus*, lane 10: *Clinostomum philippinensis*, lane 11: *Posthodiplostomum* sp.

Table 4.7 Number of fragment generated and fragment size ranged of each trematode samples based on HAT-RAPD profiles of OPA-04 primer

Lane	Trematodes	No. fragments	Size ranged (bp)
1	<i>Fasciola gigantica</i>	3	500-1000
2	<i>Paramphistomum epiclitum</i>	6	400-1200
3	<i>Fischoederius elongatus</i>	6	200-1000
4	<i>Orthocoelium streptocoelium</i>	4	250-1200
5	<i>Haplorchis taichui</i>	4	300-1000
6	<i>Stellantchasmus</i> sp.	2	300-700
7	<i>Haplorchoides</i> sp.	6	350-1500
8	<i>Opisthorchis viverrini</i>	6	400-1500
9	<i>Ganeo tigrinus</i>	1	250
10	<i>Clinostomum philippinensis</i>	3	300-1500
11	<i>Posthodiplostomum</i> sp.	6	400-1500

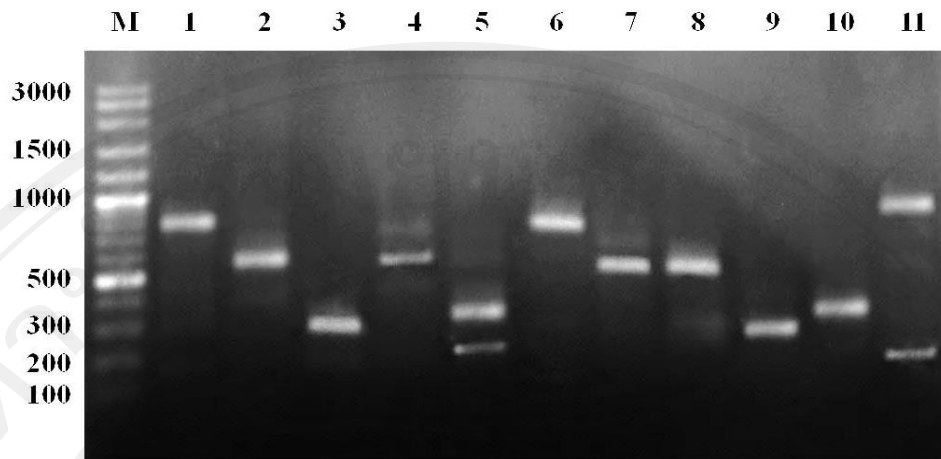


Figure 4.31 HAT-RAPD profiles generated by OPA-09 primer

Lane M: 100 bp DNA marker, lane 1: *Fasciola gigantica*, lane 2: *Paramphistomum epiclitum*, lane 3: *Fischoederius elongatus*, lane 4: *Orthocoelium streptocoelium*, lane 5: *Haplorchis taichui*, lane 6: *Stellantchasmus* sp., lane 7: *Haplorchoides* sp., lane 8: *Opisthorchis viverrini*, lane 9: *Ganeo tigrinus*, lane 10: *Clinostomum philippinensis*, lane 11: *Posthodiplostomum* sp.

Table 4.8 Number of fragment generated and fragment size ranged of each trematode samples based on HAT-RAPD profiles of OPA-09 primer

Lane	Trematodes	No. fragments	Size ranged (bp)
1	<i>Fasciola gigantica</i>	1	800
2	<i>Paramphistomum epiclitum</i>	1	600
3	<i>Fischoederius elongatus</i>	1	300
4	<i>Orthocoelium streptocoelium</i>	2	600-800
5	<i>Haplorchis taichui</i>	2	200-350
6	<i>Stellantchasmus</i> sp.	1	800
7	<i>Haplorchoides</i> sp.	1	600
8	<i>Opisthorchis viverrini</i>	1	600
9	<i>Ganeo tigrinus</i>	1	300
10	<i>Clinostomum philippinensis</i>	1	400
11	<i>Posthodiplostomum</i> sp.	2	200-1000

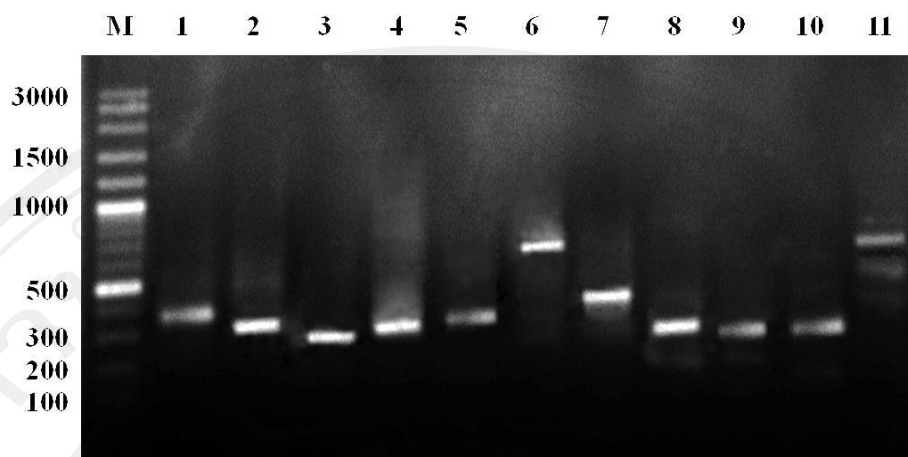


Figure 4.32 HAT-RAPD profiles generated by OPA-10 primer

Lane M: 100 bp DNA marker, lane 1: *Fasciola gigantica*, lane 2: *Paramphistomum epiclitum*, lane 3: *Fischoederius elongatus*, lane 4: *Orthocoelium streptocoelium*, lane 5: *Haplorchis taichui*, lane 6: *Stellantchasmus* sp., lane 7: *Haplorchoides* sp., lane 8: *Opisthorchis viverrini*, lane 9: *Ganeo tigrinus*, lane 10: *Clinostomum philippinensis*, lane 11: *Posthodiplostomum* sp.

Table 4.9 Number of fragment generated and fragment size ranged of each trematode samples based on HAT-RAPD profiles of OPA-10 primer

Lane	Trematodes	No. fragments	Size ranged (bp)
1	<i>Fasciola gigantica</i>	1	380
2	<i>Paramphistomum epiclitum</i>	1	350
3	<i>Fischoederius elongatus</i>	1	300
4	<i>Orthocoelium streptocoelium</i>	1	350
5	<i>Haplorchis taichui</i>	1	700
6	<i>Stellantchasmus</i> sp.	1	400
7	<i>Haplorchoides</i> sp.	1	480
8	<i>Opisthorchis viverrini</i>	1	300
9	<i>Ganeo tigrinus</i>	1	300
10	<i>Clinostomum philippinensis</i>	1	300
11	<i>Posthodiplostomum</i> sp.	2	500-700

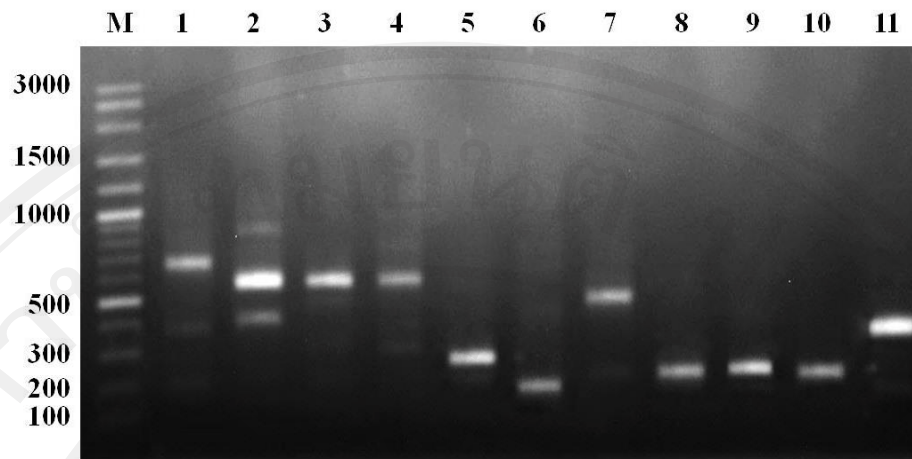


Figure 4.33 HAT-RAPD profiles generated by OPN-02 primer

Lane M: 100 bp DNA marker, lane 1: *Fasciola gigantica*, lane 2: *Paramphistomum epiclitum*, lane 3: *Fischoederius elongatus*, lane 4: *Orthocoelium streptocoelium*, lane 5: *Haplorchis taichui*, lane 6: *Stellantchasmus* sp., lane 7: *Haplorchoides* sp., lane 8: *Opisthorchis viverrini*, lane 9: *Ganeo tigrinus*, lane 10: *Clinostomum philippinensis*, lane 11: *Posthodiplostomum* sp.

Table 4.10 Number of fragment generated and fragment size ranged of each trematode samples based on HAT-RAPD profiles of OPN-02 primer

Lane	Trematodes	No. fragments	Size ranged (bp)
1	<i>Fasciola gigantica</i>	2	400-700
2	<i>Paramphistomum epiclitum</i>	3	300-900
3	<i>Fischoederius elongatus</i>	1	600
4	<i>Orthocoelium streptocoelium</i>	4	300-800
5	<i>Haplorchis taichui</i>	1	300
6	<i>Stellantchasmus</i> sp.	1	200
7	<i>Haplorchoides</i> sp.	1	500
8	<i>Opisthorchis viverrini</i>	1	250
9	<i>Ganeo tigrinus</i>	1	250
10	<i>Clinostomum philippinensis</i>	1	250
11	<i>Posthodiplostomum</i> sp.	1	400

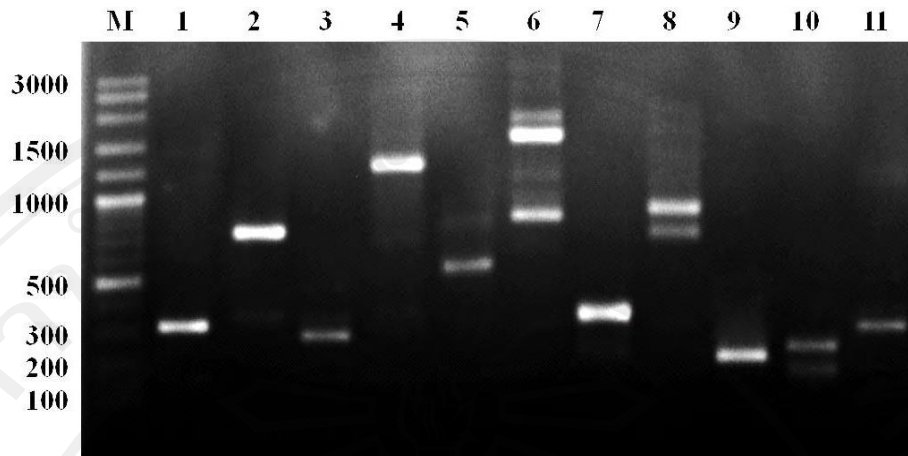


Figure 4.34 HAT-RAPD profiles generated by OPN-03 primer

Lane M: 100 bp DNA marker, lane 1: *Fasciola gigantica*, lane 2: *Paramphistomum epiclitum*, lane 3: *Fischoederius elongatus*, lane 4: *Orthocoelium streptocoelium*, lane 5: *Haplorchis taichui*, lane 6: *Stellantchasmus* sp., lane 7: *Haplorchoides* sp., lane 8: *Opisthorchis viverrini*, lane 9: *Ganeo tigrinus*, lane 10: *Clinostomum philippinensis*, lane 11: *Posthodiplostomum* sp.

Table 4.11 Number of fragment generated and fragment size ranged of each trematode samples based on HAT-RAPD profiles of OPN-03 primer

Lane	Trematodes	No. fragments	Size ranged (bp)
1	<i>Fasciola gigantica</i>	1	300
2	<i>Paramphistomum epiclitum</i>	2	350-800
3	<i>Fischoederius elongatus</i>	1	250
4	<i>Orthocoelium streptocoelium</i>	1	1400
5	<i>Haplorchis taichui</i>	2	600-800
6	<i>Stellantchasmus</i> sp.	4	900-2000
7	<i>Haplorchoides</i> sp.	1	350
8	<i>Opisthorchis viverrini</i>	2	700-900
9	<i>Ganeo tigrinus</i>	1	200
10	<i>Clinostomum philippinensis</i>	2	180-250
11	<i>Posthodiplostomum</i> sp.	1	300

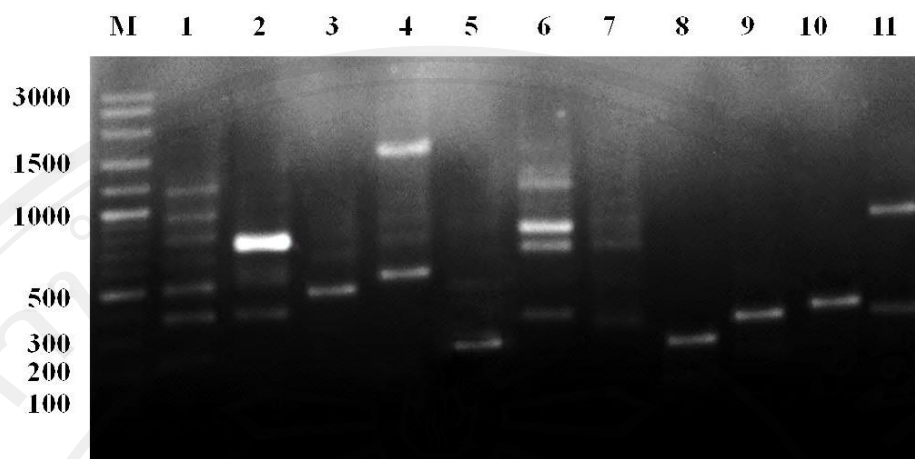


Figure 4.35 HAT-RAPD profiles generated by OPN-04 primer

Lane M: 100 bp DNA marker, lane 1: *Fasciola gigantica*, lane 2: *Paramphistomum epiclitum*, lane 3: *Fischoederius elongatus*, lane 4: *Orthocoelium streptocoelium*, lane 5: *Haplorchis taichui*, lane 6: *Stellantchasmus* sp., lane 7: *Haplorchoides* sp., lane 8: *Opisthorchis viverrini*, lane 9: *Ganeo tigrinus*, lane 10: *Clinostomum philippinensis*, lane 11: *Posthodiplostomum* sp.

Table 4.12 Number of fragment generated and fragment size ranged of each trematode samples based on HAT-RAPD profiles of OPN-04 primer

Lane	Trematodes	No. fragments	Size ranged (bp)
1	<i>Fasciola gigantica</i>	5	400-1200
2	<i>Paramphistomum epiclitum</i>	3	400-800
3	<i>Fischoederius elongatus</i>	2	500-700
4	<i>Orthocoelium streptocoelium</i>	3	600-1800
5	<i>Haplorchis taichui</i>	2	250-500
6	<i>Stellantchasmus</i> sp.	4	350-1200
7	<i>Haplorchoides</i> sp.	2	400-800
8	<i>Opisthorchis viverrini</i>	1	300
9	<i>Ganeo tigrinus</i>	1	350
10	<i>Clinostomum philippinensis</i>	1	400
11	<i>Posthodiplostomum</i> sp.	2	380-1000

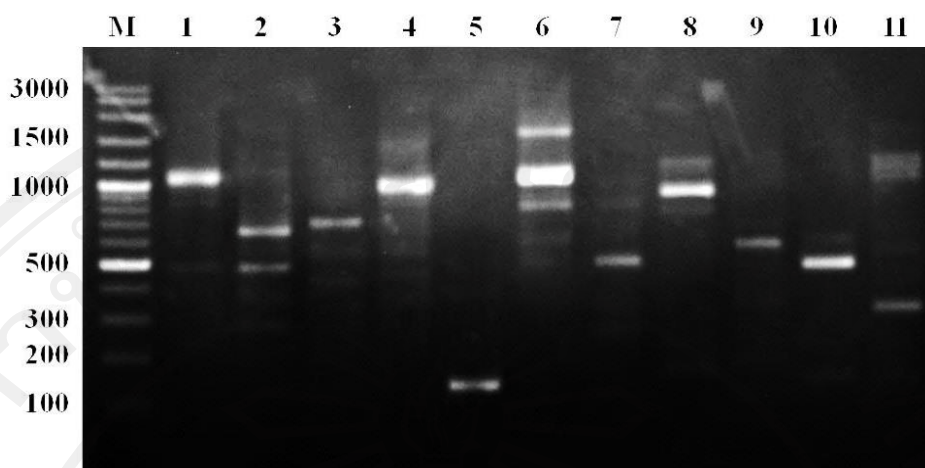


Figure 4.36 HAT-RAPD profiles generated by OPN-05 primer

Lane M: 100 bp DNA marker, lane 1: *Fasciola gigantica*, lane 2: *Paramphistomum epiclitum*, lane 3: *Fischoederius elongatus*, lane 4: *Orthocoelium streptocoelium*, lane 5: *Haplorchis taichui*, lane 6: *Stellantchasmus* sp., lane 7: *Haplorchoides* sp., lane 8: *Opisthorchis viverrini*, lane 9: *Ganeo tigrinus*, lane 10: *Clinostomum philippinensis*, lane 11: *Posthodiplostomum* sp.

Table 4.13 Number of fragment generated and fragment size ranged of each trematode samples based on HAT-RAPD profiles of OPN-05 primer

Lane	Trematodes	No. fragments	Size ranged (bp)
1	<i>Fasciola gigantica</i>	2	480-1100
2	<i>Paramphistomum epiclitum</i>	4	300-650
3	<i>Fischoederius elongatus</i>	3	400-700
4	<i>Orthocoelium streptocoelium</i>	1	1000
5	<i>Haplorchis taichui</i>	1	150
6	<i>Stellantchasmus</i> sp.	3	600-1800
7	<i>Haplorchoides</i> sp.	2	500-800
8	<i>Opisthorchis viverrini</i>	2	900-1200
9	<i>Ganeo tigrinus</i>	1	600
10	<i>Clinostomum philippinensis</i>	1	500
11	<i>Posthodiplostomum</i> sp.	2	300-1200

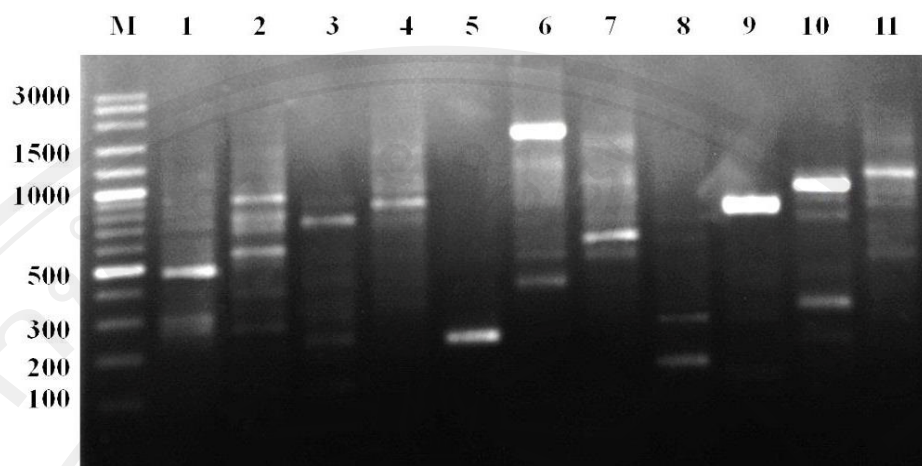


Figure 4.37 HAT-RAPD profiles generated by OPN-06 primer

Lane M: 100 bp DNA marker, lane 1: *Fasciola gigantica*, lane 2: *Paramphistomum epiclitum*, lane 3: *Fischoederius elongatus*, lane 4: *Orthocoelium streptocoelium*, lane 5: *Haplorchis taichui*, lane 6: *Stellantchasmus* sp., lane 7: *Haplorchoides* sp., lane 8: *Opisthorchis viverrini*, lane 9: *Ganeo tigrinus*, lane 10: *Clinostomum philippinensis*, lane 11: *Posthodiplostomum* sp.

Table 4.14 Number of fragment generated and fragment size ranged of each trematode samples based on HAT-RAPD profiles of OPN-06 primer

Lane	Trematodes	No. fragments	Size ranged (bp)
1	<i>Fasciola gigantica</i>	2	300-500
2	<i>Paramphistomum epiclitum</i>	6	280-900
3	<i>Fischoederius elongatus</i>	4	250-900
4	<i>Orthocoelium streptocoelium</i>	3	800-1200
5	<i>Haplorchis taichui</i>	1	250
6	<i>Stellantchasmus</i> sp.	4	500-2000
7	<i>Haplorchoides</i> sp.	4	600-1500
8	<i>Opisthorchis viverrini</i>	2	200-300
9	<i>Ganeo tigrinus</i>	1	900
10	<i>Clinostomum philippinensis</i>	4	200-1000
11	<i>Posthodiplostomum</i> sp.	4	600-1200

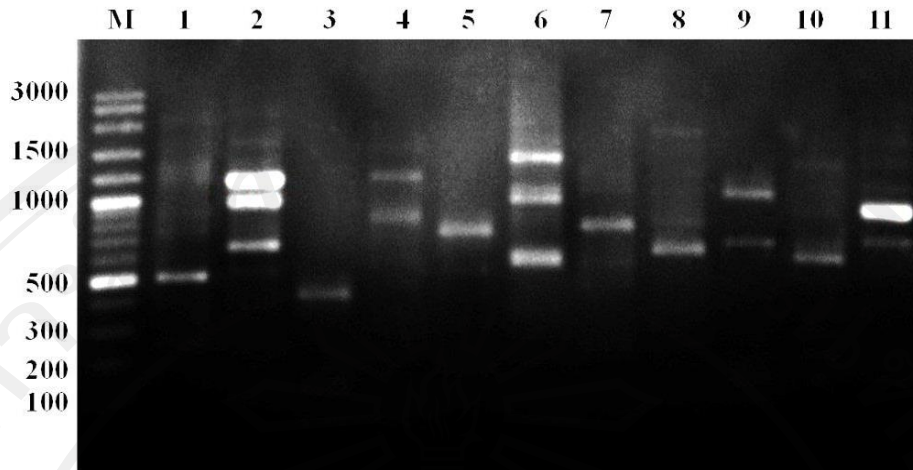


Figure 4.38 HAT-RAPD profiles generated by OPN-07 primer

Lane M: 100 bp DNA marker, lane 1: *Fasciola gigantica*, lane 2: *Paramphistomum epiclitum*, lane 3: *Fiscoederius elongatus*, lane 4: *Orthocoelium streptocoelium*, lane 5: *Haplorchis taichui*, lane 6: *Stellantchasmus* sp., lane 7: *Haplorchoides* sp., lane 8: *Opisthorchis viverrini*, lane 9: *Ganeo tigrinus*, lane 10: *Clinostomum philippinensis*, lane 11: *Posthodiplostomum* sp.

Table 4.15 Number of fragment generated and fragment size ranged of each trematode samples based on HAT-RAPD profiles of OPN-07 primer

Lane	Trematodes	No. fragments	Size ranged (bp)
1	<i>Fasciola gigantica</i>	1	550
2	<i>Paramphistomum epiclitum</i>	3	650-1200
3	<i>Fiscoederius elongatus</i>	1	400
4	<i>Orthocoelium streptocoelium</i>	2	800-1200
5	<i>Haplorchis taichui</i>	1	700
6	<i>Stellantchasmus</i> sp.	3	600-1500
7	<i>Haplorchoides</i> sp.	1	800
8	<i>Opisthorchis viverrini</i>	3	600-2000
9	<i>Ganeo tigrinus</i>	2	700-1000
10	<i>Clinostomum philippinensis</i>	1	600
11	<i>Posthodiplostomum</i> sp.	2	700-900

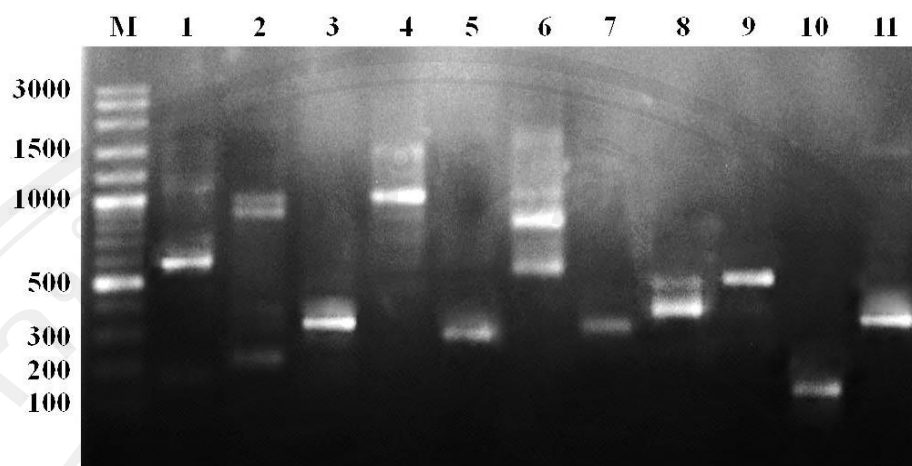


Figure 4.39 HAT-RAPD profiles generated by OPN-08 primer

Lane M: 100 bp DNA marker, lane 1: *Fasciola gigantica*, lane 2: *Paramphistomum epiclitum*, lane 3: *Fiscoederius elongatus*, lane 4: *Orthocoelium streptocoelium*, lane 5: *Haplorchis taichui*, lane 6: *Stellantchasmus* sp., lane 7: *Haplorchoides* sp., lane 8: *Opisthorchis viverrini*, lane 9: *Ganeo tigrinus*, lane 10: *Clinostomum philippinensis*, lane 11: *Posthodiplostomum* sp.

Table 4.16 Number of fragment generated and fragment size ranged of each trematode samples based on HAT-RAPD profiles of OPN-08 primer

Lane	Trematodes	No. fragments	Size ranged (bp)
1	<i>Fasciola gigantica</i>	2	600-1100
2	<i>Paramphistomum epiclitum</i>	3	250-1000
3	<i>Fiscoederius elongatus</i>	1	350
4	<i>Orthocoelium streptocoelium</i>	2	1000-1500
5	<i>Haplorchis taichui</i>	1	300
6	<i>Stellantchasmus</i> sp.	4	600-2000
7	<i>Haplorchoides</i> sp.	1	350
8	<i>Opisthorchis viverrini</i>	2	400-500
9	<i>Ganeo tigrinus</i>	1	500
10	<i>Clinostomum philippinensis</i>	1	150
11	<i>Posthodiplostomum</i> sp.	1	400

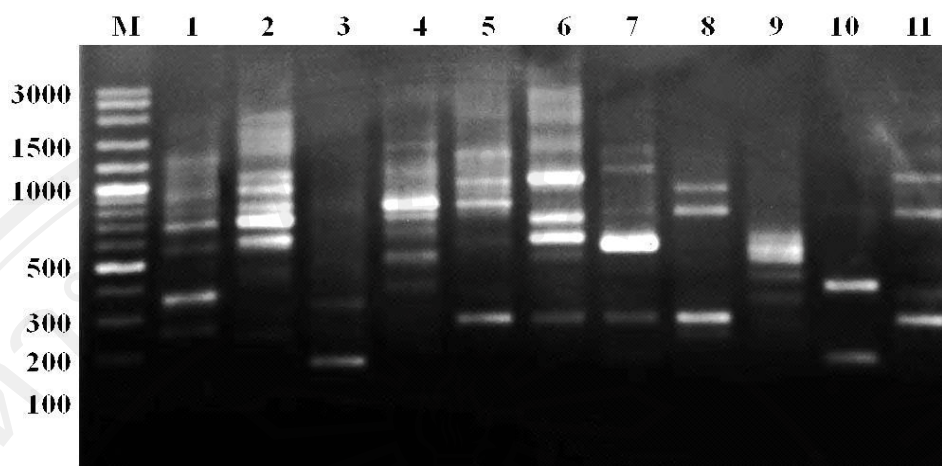


Figure 4.40 HAT-RAPD profiles generated by OPN-09 primer

Lane M: 100 bp DNA marker, lane 1: *Fasciola gigantica*, lane 2: *Paramphistomum epiclitum*, lane 3: *Fischoederius elongatus*, lane 4: *Orthocoelium streptocoelium*, lane 5: *Haplorchis taichui*, lane 6: *Stellantchasmus* sp., lane 7: *Haplorchoides* sp., lane 8: *Opisthorchis viverrini*, lane 9: *Ganeo tigrinus*, lane 10: *Clinostomum philippinensis*, lane 11: *Posthodiplostomum* sp.

Table 4.17 Number of fragment generated and fragment size ranged of each trematode samples based on HAT-RAPD profiles of OPN-09 primer

Lane	Trematodes	No. fragments	Size ranged (bp)
1	<i>Fasciola gigantica</i>	6	250-1300
2	<i>Paramphistomum epiclitum</i>	9	500-2000
3	<i>Fischoederius elongatus</i>	4	200-900
4	<i>Orthocoelium streptocoelium</i>	7	400-1500
5	<i>Haplorchis taichui</i>	5	300-1400
6	<i>Stellantchasmus</i> sp.	8	300-3000
7	<i>Haplorchoides</i> sp.	5	300-1500
8	<i>Opisthorchis viverrini</i>	3	300-900
9	<i>Ganeo tigrinus</i>	3	400-600
10	<i>Clinostomum philippinensis</i>	2	200-400
11	<i>Posthodiplostomum</i> sp.	3	300-1000

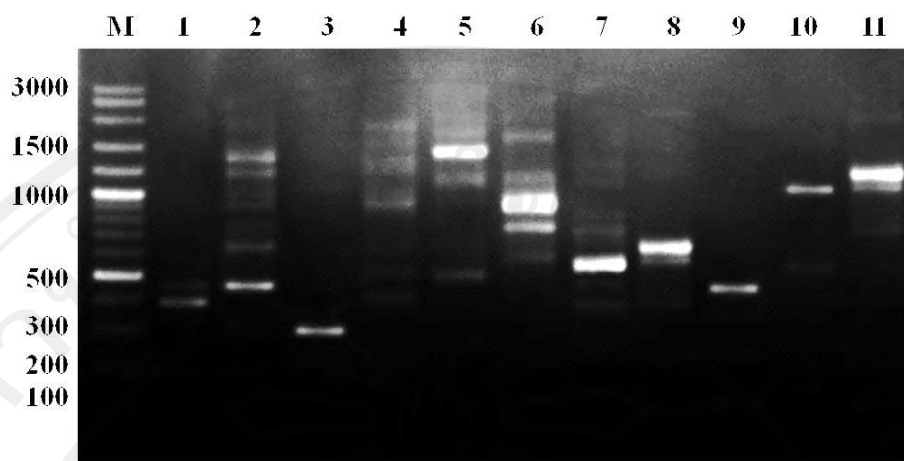


Figure 4.41 HAT-RAPD profiles generated by OPN-10 primer

Lane M: 100 bp DNA marker, lane 1: *Fasciola gigantica*, lane 2: *Paramphistomum epiclitum*, lane 3: *Fischoederius elongatus*, lane 4: *Orthocoelium streptocoelium*, lane 5: *Haplorchis taichui*, lane 6: *Stellantchasmus* sp., lane 7: *Haplorchoides* sp., lane 8: *Opisthorchis viverrini*, lane 9: *Ganeo tigrinus*, lane 10: *Clinostomum philippinensis*, lane 11: *Posthodiplostomum* sp.

Table 4.18 Number of fragment generated and fragment size ranged of each trematode samples based on HAT-RAPD profiles of OPN-10 primer

Lane	Trematodes	No. fragments	Size ranged (bp)
1	<i>Fasciola gigantica</i>	2	380-450
2	<i>Paramphistomum epiclitum</i>	5	450-1400
3	<i>Fischoederius elongatus</i>	1	300
4	<i>Orthocoelium streptocoelium</i>	6	450-2000
5	<i>Haplorchis taichui</i>	4	500-1800
6	<i>Stellantchasmus</i> sp.	5	600-1800
7	<i>Haplorchoides</i> sp.	1	600
8	<i>Opisthorchis viverrini</i>	1	600
9	<i>Ganeo tigrinus</i>	1	400
10	<i>Clinostomum philippinensis</i>	1	1000
11	<i>Posthodiplostomum</i> sp.	1	1200

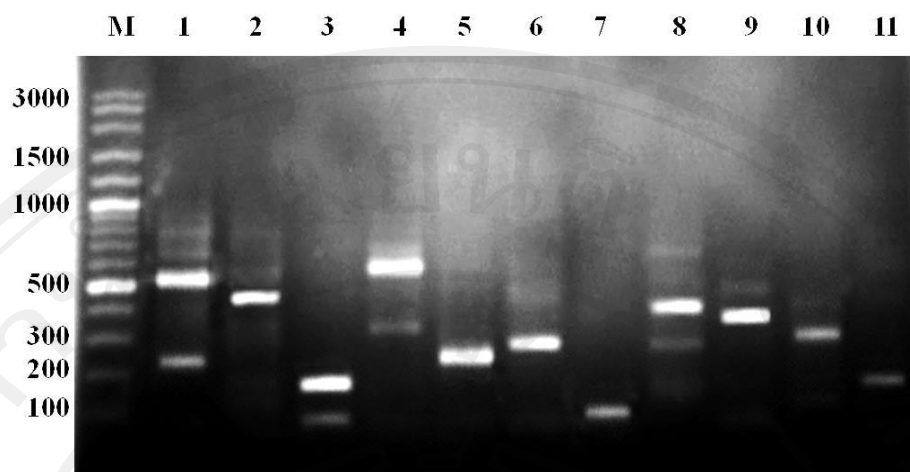


Figure 4.42 HAT-RAPD profiles generated by OPP-11 primer

Lane M: 100 bp DNA marker, lane 1: *Fasciola gigantica*, lane 2: *Paramphistomum epiclitum*, lane 3: *Fischoederius elongatus*, lane 4: *Orthocoelium streptocoelium*, lane 5: *Haplorchis taichui*, lane 6: *Stellantchasmus* sp., lane 7: *Haplorchoides* sp., lane 8: *Opisthorchis viverrini*, lane 9: *Ganeo tigrinus*, lane 10: *Clinostomum philippinensis*, lane 11: *Posthodiplostomum* sp.

Table 4.19 Number of fragment generated and fragment size ranged of each trematode samples based on HAT-RAPD profiles of OPP-11 primer

Lane	Trematodes	No. fragments	Size ranged (bp)
1	<i>Fasciola gigantica</i>	4	250-800
2	<i>Paramphistomum epiclitum</i>	1	450
3	<i>Fischoederius elongatus</i>	2	80-150
4	<i>Orthocoelium streptocoelium</i>	2	300-600
5	<i>Haplorchis taichui</i>	1	250
6	<i>Stellantchasmus</i> sp.	1	280
7	<i>Haplorchoides</i> sp.	1	100
8	<i>Opisthorchis viverrini</i>	3	280-700
9	<i>Ganeo tigrinus</i>	2	400-500
10	<i>Clinostomum philippinensis</i>	1	300
11	<i>Posthodiplostomum</i> sp.	1	150

Using a total of 16 different random arbitrary primers to randomly amplify genomic DNA from an initial 11 trematode species, a total of approximately 442 polymorphic band profiles were produced. Fragment ranging in size from 80-3000 base pairs as detailed in table 4.20.

Table 4.20 Information of primers used and total band generated, number of polymorphic including percent polymorphism of each primer

Primers	Sequences 5'-3'	Total bands	Size ranged (bp)	No. polymorphic	% polymorphism
OPA-01	TGCCGAGCTG	50	250-3000	50	100
OPA-02	TGCCGAGCTG	31	200-1500	31	100
OPA-03	AGTCAGCCAC	29	250-1500	29	100
OPA-04	AATCGGGCTG	47	200-1500	47	100
OPA-09	GGGTAACGCC	14	200-1000	14	100
OPA-10	GTGATCGCAG	12	300-700	12	100
OPN-02	ACCAGGGGCA	17	200-900	17	100
OPN-03	GGTACTCCCC	18	180-2000	18	100
OPN-04	GACCGACCCA	26	250-1800	26	100
OPN-05	ACTGAACGCC	22	150-1800	22	100
OPN-06	GAGACGCACA	35	200-2000	35	100
OPN-07	CAGCCCAGAG	20	400-2000	20	100
OPN-08	ACCTCAGCTA	19	150-2000	19	100
OPN-09	TGCCGGCTTG	55	200-3000	55	100
OPN-10	ACAACCTGGGG	28	300-2000	28	100
OPP-11	AACGCGTCGG	19	80-800	19	100
Total		442	80-3000	442	100

2) Fragment screening and sequencing of HAT-RAPD fragments

Based on DNA profiles of 16 random arbitrary primers, the expected specific bands of *F.gigantica* were approximately fragmented of 380 base pairs (bp) generated by OPN-09 primer (Fig. 4.43). This 380 bp was then purified and subjected for sequencing directly by without cloned and transformed. The nucleotide sequences were found as 334 base pairs (Fig. 4.44)

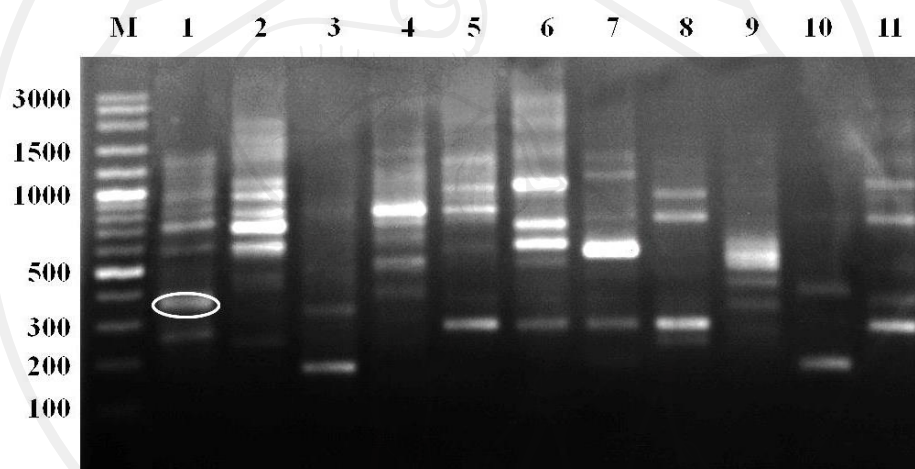


Figure 4.43 DNA profiles demonstrated that the expected approximately fragments of 380 base pairs of *F.gigantica*-specific bands generated from OPN-09 primer
Lane M: 100 bp DNA marker, lane 1: *Fasciola gigantica*, lane 2: *Paramphistomum epiclitum*, lane 3: *Fischoederius elongatus*, lane 4: *Orthocoelium streptocoelium*, lane 5: *Haplorchis taichui*, lane 6: *Stellantchasmus* sp., lane 7: *Haplorchoides* sp., lane 8: *Opisthorchis viverrini*, lane 9: *Ganeo tigrinus*, lane 10: *Clinostomum philippinensis*, lane 11: *Posthodiplostomum* sp.

```

1   GAACACAGTT CGCTGATTCT GCGAGTGCAG GGATGTCGGC ACGCTGAGGG 50
51  AGCACCAACT GAGCTTTCGA GATACCCCGA ACGAAATCAA GATCCGTTTCG 100
101 TTTTCCCCTC TGTACCTCAT GCGAGCTTTT GTATTGGTGA GCGCCACTTT 150
151 AAATTGGTGT CCCTCTTATC AATGCTAGCC TGAGGATACC GAGGGGACTA 200
201 AAGGCTGCAT CTTCTTATAT TCCGCTGTAT GTAAGAAGGT CAGCTGGTGC 250
251 TGACGTGAGG CTACGCCACT TCCAAGCATT CCGCCCCTAA GGACCACCCT 300
301 TAGGTCCATC CTGTATGGGC GAAACCCGCA AAGA----- 334

```

Figure 4.44 Illustration demonstrated nucleotide sequences of *F.gigantica*-specific (334 bp) derived from HAT-RAPD markers of OPN-09 primer

3) Designing and synthesizing of *F. gigantea*-specific primers

A pair of specific primer (forwards and reverses) was designed based on sequence data of serotype fragment that selected from RAPD markers using Primer blast (www.ncbi.nlm.nih.gov). The specific primer was designed as: FG-F (5'-TCC GTT CGT TTT CCC CTC TG-3') and FG-R (5'-GGG TTT CGC CCA TAC AGG AT-3') for *F. gigantea* with expected product size of 235 bp. Details and specific information of designed primers of *F. gigantea* were shown in figure 4.45 and table 4.21.

1 GAACACAGTT CGCTGATTCT GCGAGTGCAG GGATGTCGGC ACGCTGAGGG 50
 CTTGTGTCAA GCGACTAAGA CGCTCACGTC CCTACAGCCG TGC GACTCCC
 FG-F →
 51 AGCACCAACT GAGCTTTCGA GATACCCCGA ACGAAATCAA GATCCGTTTCG 100
 TCGTGGTTGA CTCGAAAGCT CTATGGGGCT TGCTTTAGTT CTAGGCAAGC
 101 TTTTCCCCTC TGTACCTCAT GCGAGCTTTT GTATTGGTGA GCGCCACTTT 150
 AAAAGGGGAG ACATGGAGTA CGCTCGAAAA CATAACCTCT CGCGGTGAAA
 151 AAATTGGTGT CCCTCTTATC AATGCTAGCC TGAGGATACC GAGGGGACTA 200
 TTTAACCACA GGGAGAATAG TTACGATCGG ACTCCTATGG CTCCCCTGAT
 201 AAGGCTGCAT CTTCTTATAT TCCGCTGTAT GTAAGAAGGT CAGCTGGTGC 250
 TTCCGACGTA GAAGAATATA AGGCGACATA CATTCTTCCA GTCGACCACG
 251 TGACGTGAGG CTACGCCACT TCCAAGCATT CCGCCCCTAA GGACCACCCT 300
 ACTGCACTCC GATGCGGTGA AGGTTTCGTAA GGC GGGGATT CCTGGTGGGA
 301 TAGGTCCATC CTGTATGGGC GAAACCCGCA AAGA----- 334
 ATCCAGGTAG GACATACCCG CTTTGGGCGT TTCT-----
 ← FG-R

Figure 4.45 Illustration demonstrated the designed position of the 235 bp nucleotide sequences of *F. gigantea* specific primer (red alphabet)

Table 4.21 Specification of *F. gigantea* specific primers designed by the sequences of RAPD markers of OPN-09 primer

Primers	Sequence (5'→3')	Length (bp)	T _m (°C)	GC (%)	Product (bps)
FG-F	TCCGTTTCGTTTCCCCTCTG	20	59.97	55.00	235
FG-R	GGGTTTCGCCATACAGGAT	20	59.82	55.00	

4) The specificity of *F. gigantica*-specific primers

Two pairs of designed primers were tested individually for specificity with DNA samples of related trematodes. Test of specific detection was also determined by varying the total amount of MgCl₂ and optimizing the annealing temperature until only the specific PCR product was clearly generated. The optimal PCR conditions for *F. gigantica*-specific primers performed was; 1 cycle of 94 °C for 2 minutes, 35 cycles of 94 °C for 30 seconds, 55 °C for 45 seconds, 72 °C for 1 minutes and 1 cycle of final extension at 72 °C for 7 minutes. PCR products were separated on 1.4% TBE agarose gel electrophoresis, stained with ethidium bromide, and photographed with a Kodak Digital Camera Gel Logic 100. By using common PCR composition, *F. gigantica* specific fragment was clearly generated except for the amount of MgCl₂ that was increased to 1.5 mM/reaction. The results showed that the designed specific primer can be amplified only genomic DNA of *F. gigantica*, whereas the genomic DNA of other related trematodes cannot be amplified (Fig. 4.46).

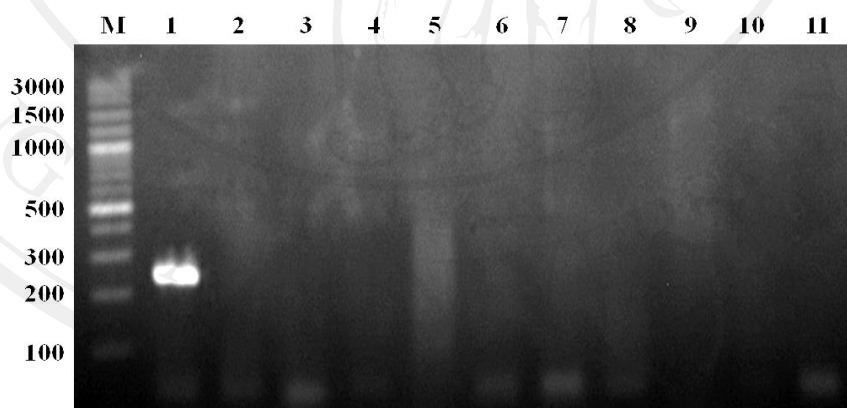


Figure 4.46 Illustration demonstrated specificity test of *F. gigantica*-specific primers
Lane M: 100 bp DNA marker, lane 1: *Fasciola gigantica*, lane 2: *Paramphistomum epiclitum*, lane 3: *Fischoederius elongatus*, lane 4: *Orthocoelium streptocoelium*, lane 5: *Haplorchis taichui*, lane 6: *Stellantchasmus* sp., lane 7: *Haplorchoides* sp., lane 8: *Opisthorchis viverrini*, lane 9: *Ganeo tigrinus*, lane 10: *Clinostomum philippinensis*, lane 11: *Posthodiplostomum* sp.

5) Reaction sensibility of *F. gigantica*-specific primers

The sensibility of *F. gigantica*-specific primers was determined by varying the concentration of DNA template of adult stage, which it is serially diluted in 10 folds. The initial concentration used was 50 ng and serially diluted to 5 ng, 500 pg, 50 pg and 5 pg respectively. In the results showed that the intensity of 235 bp specific bands was gradually decreased as depended on the decreasing of template concentration. The lowest concentration of DNA template that could be amplified by using the specific primers in PCR reaction was approximately at 50 pg (Fig. 4.47).

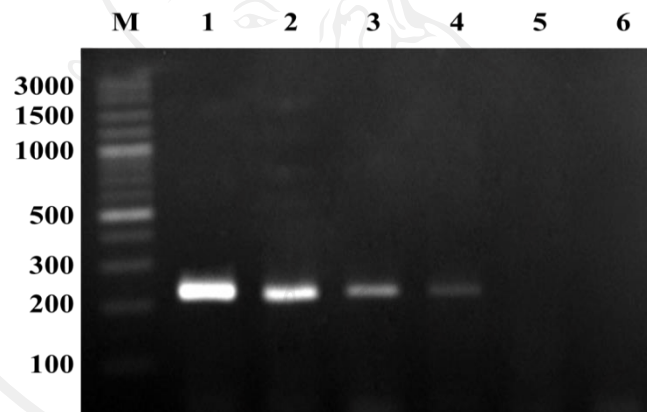


Figure 4.47 Illustration demonstrated the reaction sensibility of *F. gigantica*-specific primers based on 10 folds serial dilution method; Lane M: 100 bp DNA marker, lane 1: 50 ng, lane 2: 5 ng, lane 3: 500 pg, lane 4: 50 pg, lane 5: 5 pg

6) Specificity test on experimental larval stages of *F. gigantica*

All experimental larval stages of *F. gigantica* such as miracidium, sporocyst, redia, cercaria, metacercaria, were individually extracted for genomic DNA and then all genomic DNA were tested with *F. gigantica*-specific primers. The results showed that *F. gigantica*-

specific primer can be amplified in genomic DNA of all larval stages (Fig. 4.48).

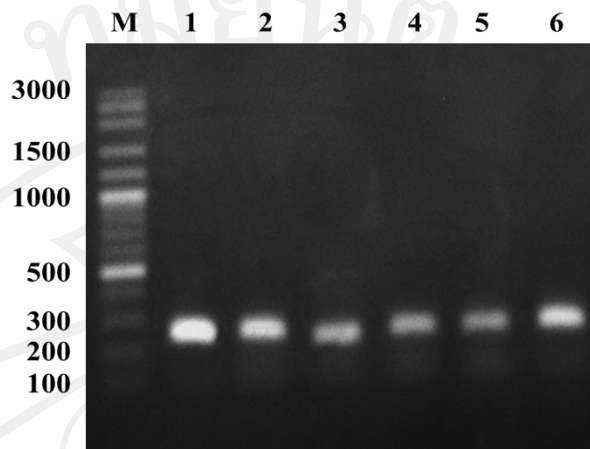


Figure 4.48 Illustration demonstrated the reaction specificity of *F. gigantica*-specific primers that were amplified with different *F. gigantica* experimental larval stages; Lane M: 100 bp DNA marker, lane 1: adult, lane 2: *miracidium*, lane 3: sporocyst, lane 4: redia, lane 5: cercaria, lane 6: metacercaria

7) Specificity on field-collected samples of larval stages

The 8 types of cercariae as parapleurolophocercous cercaria, pleurolophocercous cercaria, monostome cercaria, distome cercaria, xiphidiocercaria, echinostome cercaria, transversotremacercaria and furcocercous cercaria found in field-collected snail samples from Chiang Mai province were extracted for genomic DNA. All genomic DNA of each cercarial type were amplified with *F. gigantica*-specific primers and resulted that, the 235 bp specific band was generated in only *F. gigantica* control sample. Whereas samples of all cercarial DNA were not be amplified. It can be confirmed that all cercarial types found in fields-collected snails are not the cercariae of *F. gigantica* (Fig. 4.49).

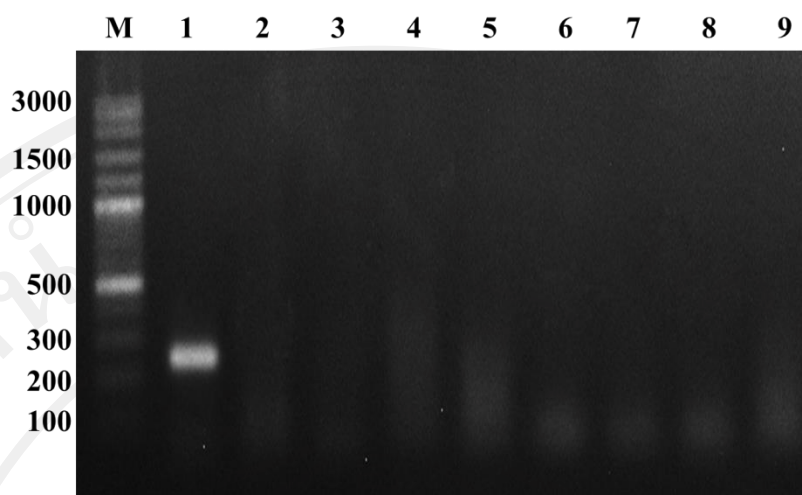


Figure 4.49 Illustration demonstrated the specific confirmation of *F. gigantica* on different cercariae samples harvested from field-collected snails; Lane M: 100 bp DNA marker, lane 1: *F. gigantica* (control group), lane 2: parapleurolophocercous cercaria, lane 3: pleurolophocercous cercaria, lane 4: monostome cercaria, lane 5: distome cercaria, lane 6: xiphidiocercaria, lane 7: echinostome cercaria, lane 8: transversotremacercaria, lane 9: furcocercous cercaria

4.5.2 Phylogenetic study

1) Amplification of Internal Transcribed Spacer subunit 2 (ITS 2) region

ITS-2 sequences of *F. gigantica* were comparative analyzed with related trematodes species that available in Genbank. Supplemented fluke samples such as; *F. gigantica* (Vietnam), *Fishoederius elongatus*, *Paramphistomum epiclitum*, *Orthocoelium streptocoelium*, *Haplorchis taichui*, *Stellantchasmus* sp., *Haplorchoides* sp., *Opisthorchis viverrini* were also included. PCR products of ITS-2 region generated by primer 3S-F (forward primer) and BD2-R (reverse primer) were found approximately 500 bp. A few over hanging in fragment sizes between species were also found (Fig. 4.50).

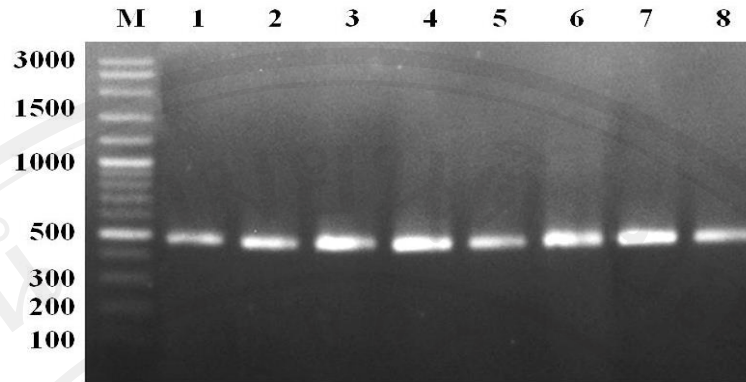


Figure 4.50 DNA profiles of ITS-2 region derived from BD2-R and 3S-F primer; Lane M: 100 bp DNA marker, lane 1: *Fasciola gigantica*, lane 2: *Fishoederius elongatus*, lane 3: *Paramphistomum epiclitum*, lane 4: *Orthocoelium streptocoelium*, lane 5: *Haplorchis taichui*, lane 6: *Stellantchasmus* sp., lane 7: *Haplorchoides* sp., lane 8: *Opisthorchis viverrini*

Then, all PCR products were purified and subjected for sequencing directly by without cloned and transformed. Sequences alignment of *F. gigantica* found in this study demonstrated the maximum length obtained was 533 base pairs (Fig. 4.51).

```

1   GCGGATTAAT ATTGAGTGAG CATACTGTGT GATTAATGCA AACTGCATAC 50
51  TGCTTTGAAC ATCGACATCT TGAACGCATA TTGCGGCCAT GGGTTAGCCT 100
101 GTGGCCACGC CTGTCCGAGG GTCGGCTTAT AAACATCAC GACGCCCAA 150
151 AAGTCGTGGC TTGGGTTTTG CCAGCTGGCG TGATCTCCTC TATGAGTAAT 200
201 CATGTGAGGT GCCAGATCTA TGGCGTTTCC CTAATGTATC CGGATGCACC 250
251 CTTGTCTTGG CAGAAAGCCG TGGTGAGGTG CAGTGGCGGA ATCGTGGTTT 300
301 AATAATCGGG TTGGTACTCA GTTGTCACTG TGTTCGGCGA TCCCCTAGTC 334
351 GGCACACTCA TGATTTCTGG GATAATTCCA TACCAGGCAC GTTCCGTTAC 400
401 TGTTACTTTG TCATTGGTTT GATGCTGAAC TTGGTCATGT GTCTGATGCT 450
451 ATTTCATATA ACGACGGTAC CCTTCGTGGT CTGTCTTCCT GACCTCGGTT 500
501 CAGACGTGAT TACCCGCTGA ATTTAAGAAT AAA----- 533

```

Figure 4.51 Illustration demonstrated 533 ITS2 nucleotide sequences data of *F. gigantica*

2) Data analysis

Based on the ITS-2 sequence data, they were then aligned and compared with 12 accession numbers of *F. gigantea* ITS-2 sequences including *F. hepatica* that available in NCBI-GenBank and some supplemented fluke species (this study). The result showed that *F. gigantea* found in this study revealed 98-99% maximum identities as demonstrated in table 4.22.

Table 4.22 The maximum identities and query coverage of *F. gigantea* in this study compared with closely related-trematodes available in NCBI-GenBank

Accession	Geographical location	Query coverage	Maximum identity
HQ700438.1	China	95%	99%
AB536921.1	Viet Nam	95%	99%
AB553695.1	Egypt	95%	99%
JF930346.1	India	95%	99%
AB010977.1	Indonesia	93%	99%
AB010979.1	Japan	93%	99%
AB010976.1	Zambia	93%	99%
JN828958.1	Iran	85%	99%
AM850108.1	Niger	87%	99%
AB207149.1	Thailand	93%	99%
JF432078.1	Iran	86%	98%
JF708029.1	USA	87%	98%

The comparative study of ITS2 sequences among *F. gigantea* obtained in this study with closely related samples in NCBI-GenBank, and 7 supplemented trematodes; *Haplorchis taichui*, *Stellantchasmus* sp., *Haplorchoides* sp., *Opisthorchis viverrini*, *Fishoederius elongatus*, *Paramphistomum epiclitum* and *Orthocoelium streptocoelium* as an out group was analyzed the phylogenetic relationships. Maximum likelihood (ML) and UPGMA methods with bootstrap values of 1000 replicates set were performed the phylogenetic tree. The results showed that, 4 groups of trematodes were generated, first was *F.gigantica* group including the specimen of Chiang Mai, second was 2 samples of *F. hepatica* (GenBank), third was group of 3 rumen flukes; *Fishoederius elongatus*, *Paramphistomum epiclitum* and *Orthocoelium streptocoelium* (this study) and fourth was group of 3 minute intestinal flukes; *Haplorchis taichui*, *Stellantchasmus* sp., *Haplorchoides* sp. and liver fluke; *Opisthorchis viverrini*, respectively (Figs. 4.52-4.53). These results can be confirmed that the Giant liver fluke which mainly caused fascioliasis in Chiang Mai province, Thailand was identified as *F. gigantea*.

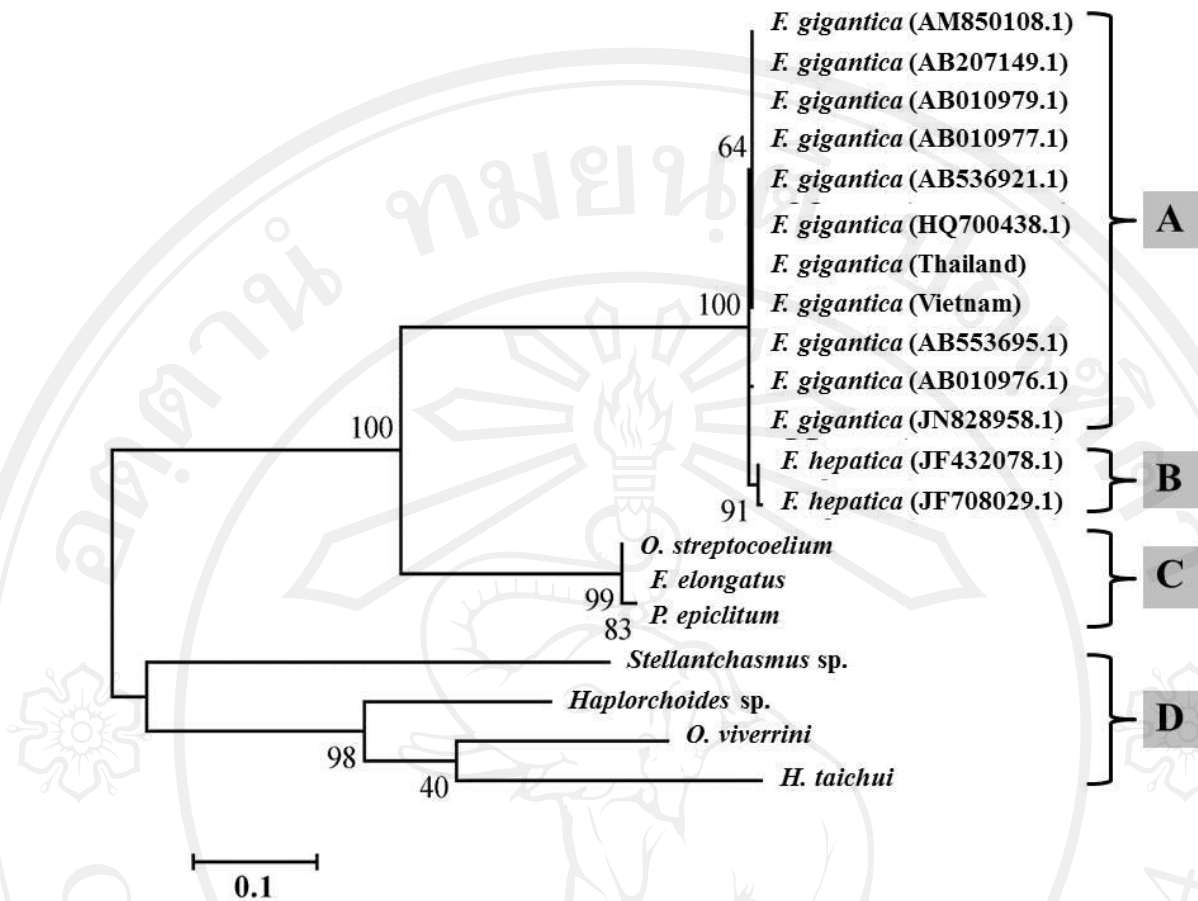


Figure 4.52 Phylogram derived from maximum likelihood analysis depicting phylogenetic relationships of trematodes used in this study by basing on ITS-2 sequences; (A): group of *F.gigantica* obtained from both Chiang Mai and GenBank, (B): group of *F. hepatica* (GenBank), (C): group of rumen flukes (*Orthocoelium streptocoelium*, *Fishoederius elongatus* and *Paramphistomum epiclitum*) and (D): group of minute intestinal fluke (*Haplorchis taichui*, *Stellantchasmus* sp., *Haplorchoides* sp.) and liver flukes (*Opisthorchis viverrini*)

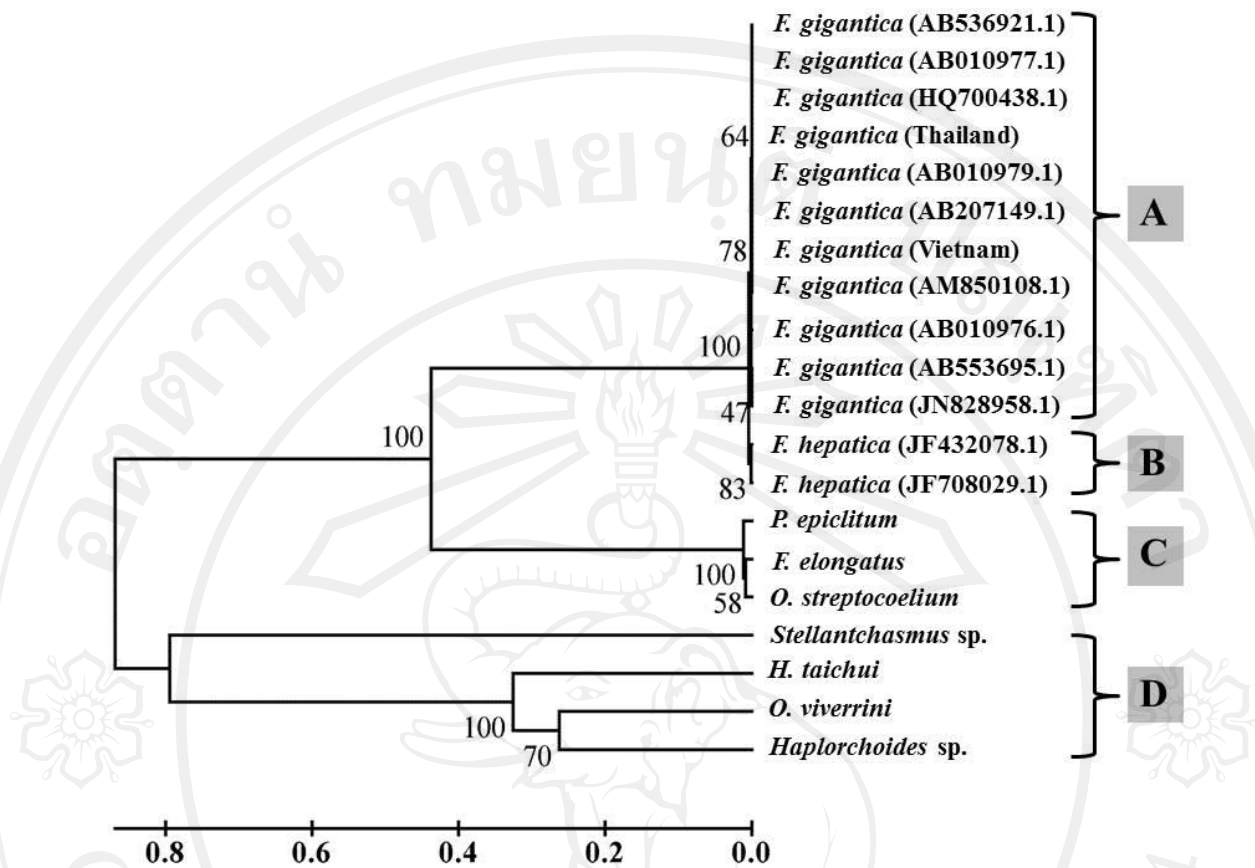


Figure 4.53 Phylogram derived from an UPGMA analysis depicting phylogenetic relationships of trematodes used in this study by basing on ITS2 sequence data; (A): group of *F.gigantica* obtained from both Chiang Mai and GenBank, (B): group of *F. hepatica* (GenBank), (C): group of rumen flukes (*Orthocoelium streptocoelium*, *Fishoederius elongatus* and *Paramphistomum epiclitum*) and (D): group of minute intestinal fluke (*Haplorchis taichui*, *Stellantchasmus* sp., *Haplorchoides* sp.) and liver flukes (*Opisthorchis viverrini*)

The genetic diversity of *F. gigantea* in this study compared with *F. gigantea* and *F. hepatica* that available in GenBank. The results revealed that *F. gigantea* in this study are same species with other countries ($K < 4\theta$) while, *F. gigantea* difference from *F. hepatica* ($K > 4\theta$) (Table 4.23).

Table 4.23 The variables speciation of genetic diversity of *F. gigantea* and *F. hepatica*

Population	Nucleotide diversity (π)	θ	$\theta \times 4$	Sequence divergence between clades (K)	K \geq 4?
<i>F. gigantea</i>	0.00242	0.00251	0.01004	0.00142	No
<i>F. hepatica</i>	0.00236	0.00236	0.00944	0.01071	Yes